Genomic and metabolomic insights into the modes-of-action of bacterial strains to control the grapevine wood pathogen, Fomitiporia mediterranea

Ouiza Mesguida, Stéphane Compant, Adrian Wallner, Livio Antonielli, Ryszard Lobinski, Simon Godin, Mickael Le Béchec, Maxence Terrasse, Ahmed Taibi, Assia Dreux-Zigha, et al.

Microbiological Research 293 (2025) 128085

Contents lists available at ScienceDirect

Microbiological Research

journal homepage: www.elsevier.com/locate/micres

Genomic and metabolomic insights into the modes-of-action of bacterial strains to control the grapevine wood pathogen, *Fomitiporia mediterranea*

Ouiza Mesguida [a,b,*], Stéphane Compant [c], Adrian Wallner [c], Livio Antonielli [c], Ryszard Lobinski [a,d], Simon Godin [a], Mickaël Le Bechec [a], Maxence Terrasse [a], Ahmed Taibi [b], Assia Dreux-Zigha [b], Jean-Yves Berthon [b], Rémy Guyoneaud [a,1], Patrice Rey [a,1], Eléonore Attard [a,1]

[a] Universite de Pau et des Pays de l'Adour, CNRS, IPREM, Pau, France
[b] GreenCell: Biopôle Clermont-Limagne, Saint Beauzire 63360, France
[c] Center for Health & Bioresources, Bioresources Unit, AIT Austrian Institute of Technology, Konrad Lorenz Str. 24, Tulln 3430, Austria
[d] Chair of Analytical Chemistry, Warsaw University of Technology, Warsaw 00-664, Poland

ARTICLE INFO

Keywords:
Esca
Pseudomonas
Paenibacillus
Genes clusters
Antifungal metabolites

ABSTRACT

Grapevine trunk diseases (GTDs), particularly Esca, represent a major challenge for viticulture worldwide, leading to substantial economic losses. With no effective control treatments available, developing new methods such as biocontrol is crucial for managing GTDs. Our aim was to select biocontrol bacteria effective against the white-rot fungal pathogen *Fomitiporia mediterranea* (Fmed) and to investigate their mechanisms of action. A stepwise screening of 58 bacterial strains was conducted *in vitro* to assess their ability to inhibit Fmed growth through volatile and diffusible metabolites production. The screening was also done on wood sawdust from seven different grapevine cultivars. Out of 58 tested strains, 49 inhibited Fmed growth by over 50 % through their volatile organic compounds, only eight achieving this through their agar-diffusible metabolites. *Pseudomonas lactis* SV9, *Pseudomonas paracarnis* S45, and *Paenibacillus polymyxa* SV13 exhibited a strong efficacy in inhibiting Fmed on wood sawdust in a cultivar-dependent manner. We selected these strains for whole genome analysis and metabolomic profiling via LC-MS/MS for diffusible compounds and SPME GC-MS for volatile compounds. *P. polymyxa* SV13 inhibited Fmed primarily through diffusible metabolites, producing mainly fusaricidin-type compounds. Conversely, *Pseudomonas* strains acted mainly via their volatile metabolites, producing mainly the antifungal compound dimethyl disulfide. Genome analysis of the three bacterial strains revealed gene clusters responsible for regulating both direct and indirect mechanisms in biocontrol agents (BCAs). Our findings highlight the importance of comprehensive studies that combine *in vitro* experiments mimicking field conditions, with detailed investigations into modes of action to improve BCAs efficacy.

1. Introduction

Viticulture plays a major role in agriculture contributing considerably to the economy of several countries. However, grapevine trunk diseases (GTDs), mainly Esca, are currently among the most important challenges for viticulture in the world (Mondello et al., 2018a). Esca causes significant economic losses throughout the viticulture sector by decreasing vineyard longevity and affecting wine quality (Fontaine et al., 2016). While sodium arsenate was highly effective in controlling Esca, it was banned in Europe in 2003 due to its toxicity. Since then, Esca has re-emerged and became a major concern for the wine industry in many wine regions around the world.

Esca is a complex disease caused by several pathogenic fungi, mainly the ascomycetes, *Phaeomoniella chlamydospora* and *Phaeoacremonium minimum* and the basidiomycete *Fomitiporia mediterranea* (Fmed) (Bertsch et al., 2013; Mondello et al., 2018b). Fmed is a wood-decaying basidiomycete associated with Esca of grapevine in Europe and Mediterranean regions, and the primary basidiomycete responsible for the white rot (Fischer, 2002; Moretti et al., 2021). It is generally assumed that the wood colonizing pathogens, *P. chlamydospora* and *P. minimum*

* Corresponding author at: E2S UPPA, CNRS, IPREM, Université de Pau et des Pays de l'Adour, Pau 64000, France.
E-mail address: ouiza.mesguida@univ-pau.fr (O. Mesguida).
[1] Co-last authors

https://doi.org/10.1016/j.micres.2025.128085
Received 29 September 2024; Received in revised form 16 January 2025; Accepted 24 January 2025
Available online 30 January 2025

act as precursors and cause initial wood degradation, which facilitates Fmed to complete wood degradation with the formation of white rot necrosis (Bruez et al., 2014; Haidar et al., 2021; Surico et al., 2006; Valtaud et al., 2009). Here, we focus on Fmed because numerous authors have suggested a strong connection between white rot necrosis, the congruent presence of Fmed and the development of Esca symptoms (Ouadi et al., 2021; Bruez et al., 2020). Ouadi et al. (2021), reported that in 17-year-old Cabernet Sauvignon grapevines exhibiting Esca foliar symptoms, at least 10 % of plants had been affected by white rot. On 10-year-old diseased grapevines of the same cultivar, Bruez et al. (2020) demonstrated that the most abundant pathogens in white rot necrosis were Fmed and *P. chlamydospora*, with Fmed being far more abundant than *P. chlamydospora* (relative abundances between 60 % and 90 % for Fmed, and 5–15 % for *P. chlamydospora*). Regarding bacteria, their interactions with fungi have a major influence on plant health, either by promoting the degradation of wood components, or by preventing it. Haidar et al. (2021, 2024) have shown that *Paenibacillus* spp. interact synergistically with Fmed accelerating the wood degradation.

On the other hand, numerous microorganisms that colonize wood tissues inhibit Fmed development. For instance, fungal strains belonging to the genera *Aphanocladium, Epicoccum*, *Pleurotus* and *Trichoderma* were evaluated in dual culture assays against Fmed, and caused a significant reduction in Fmed growth (Del Frari et al., 2019; Mannerucci et al., 2023; Riedle-Bauer et al., 2023). Riedle-Bauer et al. (2023) used grapevine wood discs and showed that *Trichoderma* strains completely inhibited Fmed growth. Furthermore, other bacterial strains inhibit Fmed growth and can be used as biocontrol agents against Fmed. Strains belonging to the genera *Bacillus*, *Novosphingobium*, *Pseudomonas* and *Stenotrophomonas* have been shown to inhibit the development of Fmed *in vitro* (Haidar et al., 2021; Riedle-Bauer et al., 2023). Despite the few studies conducted on the antagonistic activity of bacteria isolated from grapevines against Fmed, further research is needed to explore the potential of these biocontrol agents, especially to understand their mechanisms of action against Fmed.

Even though Esca is one of the oldest diseases of grapevine (Bruno et al., 2020), no effective chemical products are available to control it in vineyards. One control method consists in sound crop management, such as pruning or grapevine curettage (Cholet et al., 2021) on Esca diseased plants. For instance, curettage decreased plant mortality, restored plant vigor and increased production and grape quality (Cholet et al., 2021). However, this method is not often set up in vineyards, as it requires strong technical knowledge and sound practice to cure plants effectively, without disrupting the sap flow.

In this context, bacteria isolated from grapevines tissues have emerged as a promising alternative, offering a sustainable biocontrol strategy that harnesses natural microbial interactions within the plant. The underlying idea is therefore to use bacteria that naturally colonize grapevines, as they are adapted to growing on and within this plant. Knowing the key role of Fmed in Esca disease, our study aims to isolate bacterial grapevine endophytes having antagonistic activities against this pathogenic fungus. Additionally, we aim to identify their mechanisms of action using genomic and metabolomic approaches to promote the development of innovative, eco-friendly solutions for managing Esca disease in grapevines.

2. Materials and methods

2.1. Fungal isolates

Six *F. mediterranea* isolates were selected for this study. They were obtained from INRAE-UMR 1065 SAVE collection and isolated from trunk necrosis from French vineyards. The two strains, Ph CO 36 and CO31, were isolated from the Ugni Blanc cultivar; strains SO21 and SO71 were obtained from Cabernet Sauvignon, while strain SO70 was isolated from Cabernet Franc the strain SO23 was isolated from the Sauvignon cultivar. These strains were cultivated on Malt Agar medium and incubated for 15 days at 28 °C before being used in *in vitro* tests.

2.2. Bacterial strains

We used 58 bacterial strains from the collection of UMR SAVE, INRAE, Bordeaux. Thirty-three of them were isolated from the woody tissues of Esca symptomatic grapevines of Sauvignon Blanc (Haidar et al., 2021). Twenty-five were obtained from Cabernet Sauvignon (Bordeaux vineyards) and Ugni Blanc sap (Cognac vineyards). Bacterial strains were identified by sequencing the 16S rRNA gene using the primers 799 f and 1492r (Eurofins, France). They were grown on TSA (Trypticase Soy Agar) at 28 °C.

2.3. Enzymatic assays for wood degradation

Wood degradation was studied via the ability of the 58 bacterial strains to grow on three selective media containing cellulose, lignin or xylan (hemicellulose) at 28 °C for seven days in the dark.

(i) CMC medium contained carboxymethylcellulose as a sole carbon source [1 g/l K_2HPO_4; 1 g/l $(NH_4)_2SO_4$; 0.5 g/l $MgSO_47H_2O$; 0.5 g/l NaCl; 5 g/l sodium of carboxymethylcellulose (CMC, Sigma); and 20 g/l of agar pH = 5] (Ulrich et al., 2008).
(ii) Xylan medium contained xylan beechwood as the sole carbon source [1 g/l K_2HPO_4; 1 g/l $(NH_4)_2SO_4$; 0.5 g/l $MgSO_47H2O$; 0.5 g/l NaCl; 5 g/l beechwood xylan (Apollo Scientific); and 20 g/l of agar; pH= 5] (Alexander and Zuberer, 1991).
(iii) RBBR (Remazol Brilliant Blue R) medium contained 0.05 % RBBR (Sigma) [1 g/l NaCl; 0.1 g/l of yeast extract; 1.95 g/l MES (Sigma); and 20 g/l agar] (Ulrich et al., 2008).

Xylanolytic and cellulolytic activities were detected using 0.1 % Congo red, staining for 40 min followed by a counter-coloration using 1 M NaCl (Teather, Wood, 1982). The ligninolytic activity was indicated by RBBR medium color from blue to pale pink when positive (Murray and Woodward, 2007). Each enzymatic activity was measured according to the size (mm) of the discoloration/coloration zones formed around the bacterial colonies. The degradation is classified as moderate (5–40 mm), strong (41–70 mm), and very strong (>71 mm) (Haidar et al., 2021). Four replications were performed for each strain and each medium.

2.4. Antagonistic activity: dual culture assays for inhibition of Fmed by bacteria

2.4.1. Inhibition by direct confrontation

During seven days at 28 °C a mycelial plug of Fmed Ph CO 36 was cultivated in the center of Malt Agar plates. The bacterial strains were grown over night on TSA at 28 °C, then were streaked at the edge of each plate with Fmed. The plates were then incubated in the dark at 28 °C.

2.4.2. Inhibition by indirect confrontation

For volatile organic compounds assays (VOCs), the bottom parts of two Petri plates, one with a 1-week culture of Fmed Ph CO 36 on malt agar and one with a fresh culture of each bacterial strain (TSA) were placed face-to-face with the bacterial culture on the bottom, and the pathogen culture at the top. The plates were then sealed with parafilm and incubated in the dark at 28°C. The control plates consisted of Fmed plate inverted over sterile TSA medium.

For both assays, the inhibition of Fmed growth by the bacterial isolates was assessed by measuring the radius of the colony in mm compared to the control after seven days of the coculture (Haidar et al., 2021). In details the mycelial growth inhibition percentage (GI%) was calculated using the following equation: GI% = 100 x (R2 - R1)/R2. R1 is the radial distance (mm) grown by Fmed in the direction of the bacterial strain and R2 is the radial distance (mm) grown by the Fmed in the

opposite direction for the direct confrontation assay. In the VOCs assay, R1 represents the radial colony diameter (mm) of the pathogen on plates faced to the bacterial cultures, while R2 indicates the radial growth of the pathogen on plates faced to TSA medium (control). Four biological replicates were performed for each bacterial strain/Fmed combination and for the control.

To determine to what extent our results from one strain of Fmed can be generalized to the diversity of Fmed strains in nature we selected 15 bacterial strains (five from wood and 10 from sap) to be tested against five additional Fmed strains. These simultaneously most efficient Ph CO 36 inhibitors and weakest wood degraders were selected for downstream procedures.

2.5. Antagonistic activity: wood microcosms for inhibition of Fmed by bacteria

To be used as a more realistic cultivation media, pruning wood and healthy wood of trunk (7-year-old cultivar Ugni Blanc from Cognac vineyard, France) was dried and ground to 1 mm chips, and then sterilized twice for 20 min at 120 °C, with an interval of two days in between.

Petri plates, each containing 2 g of sterile pruning or trunk wood sawdust, were inoculated with a mycelial plug of Fmed Ph CO 36. The plates were then incubated for one week at 28 °C with 3 mL of sterile distilled water. The bacterial strains were grown overnight in TSB (Tryptic Soy Broth) (28 °C, 200 rpm), then centrifuged twice at 5000 g, 5 min each time. The concentration of the bacteria was standardized at 0.1 OD in sterile physiological water (OD = 0.1 ~ 10^8 CFU/mL). Four mL of the bacterial suspension were added to the one-week culture of Fmed. The control plates consisted of 1-week Fmed culture on which 4 mL of sterile physiological water were added. The mycelial growth of Fmed was assessed by measuring (i) the radius of the colony in mm and (ii) mycelium density after seven, 14 and 21 days of incubation at 28°C. The mycelial growth inhibition was calculated with respect to the control, using the following equation: GI% = 100 x (R2 - R1)/R2. Four biological replicates were performed for each bacterial strain/Fmed combination and for the control.

To evaluate the variability in the efficacy of a given bacterial strain across different cultivars, the bacterial strains with the most efficient inhibition of Fmed Ph CO 36 on wood sawdust from the cultivar Ugni Blanc, were selected for further antagonism studies on microcosms of six grapevine cultivars including: Baroque (BRQ), Cabernet Franc (CF), Cabernet Sauvignon (CS), Gros Manseng, (GM), Fer Servadou (FS) and Sauvignon Blanc (SB) originating from the Tursan Vineyards near Pau, France.

In these experiments, we studied the antagonistic activity of selected bacteria using the same protocol as described above for curative application assays. We then evaluated the ability of these bacteria to prevent wood colonization by Fmed using the following procedure: in Petri plates containing 2 g of sterile wood sawdust from each cultivar, we inoculated 4 mL of a bacterial suspension prepared in sterile physiological water at 10^8 CFU/mL, prepared from an overnight culture in TSB (28 °C, 200 rpm). The plates were incubated for three days at 28°C. On the third day, a plug of Fmed Ph CO 36 was added to the center of each plate. For the control, a Fmed plug was added to wood sawdust inoculated with sterile physiological water. The plates were then incubated at 28 °C for three weeks. Mycelial growth of Fmed was assessed by measuring (i) the radius of the colony in mm and (ii) mycelium density after seven, 14, and 21 days, which was assessed using a scale from 1 to 5, with 1 representing the plate with the lowest density and 5 indicating the highest density observed. Five biological replicates were performed for each condition.

2.6. Genome sequencing and assembly

To sequence the whole genome of the three bacterial strains the bacterial DNA was extracted using the DNA extraction kit DNeasy® UltraClean® Microbial Kit following the manufacturer's instructions. Whole genome sequencing was performed at Eurofins Genomics GmbH (Konstanz, Germany) using the Illumina NovaSeq 6000 platform, with an S4 flowcell and sequencing mode PE150 XP. Genome sequences, along with related metadata, are available on NCBI under the BioProject PRJNA1105748. The BacFlux workflow v1.1.2 was used for quality control, adapter trimming, genome assembly, contaminant inspection, genome completeness evaluation, taxonomic assignment, antimicrobial resistance and virulence gene screening, as well as plasmid and phage investigation (Antonielli et al., 2024).

2.7. Annotation and comparative genomic analysis

Functional annotation of the three genomes, was performed using the Classic RAST (Rapid Annotation using Subsystem Technology) web server (http://rast.nmpdr.org) (Aziz et al., 2008) and the hierarchical orthology framework EggNOG 4.5 (Huerta-Cepas et al., 2016). Antimicrobial resistance (AMR) gene sequences were identified by mapping quality-filtered reads (processed using fastp v0.23.4) from the whole-genome sequencing to the Comprehensive Antibiotic Resistance Database (CARD v3.2.9) using BBMap v39.06, with a minimum identity threshold of 99 %. Features with a covered length of at least 70 % were considered as a match, according to the EFSA criteria (European Food Safety Authority (EFSA (EFSA, (2024)). Putative genes for carbohydrate active enzymes (CAZymes) were classified by dbCAN2 based on the HMMER database (Lombard et al., 2014). Biosynthetic gene clusters and secondary metabolites were predicted using antiSMASH version 7.1.0 (Blin et al., 2023). The three genomes were also annotated by comparing the DIAMOND+MEGAN pipeline analysis (Bağcı, et al., 2021) to the PLaBAse database for the identification of potential PGPT genes (Patz et al., 2024).

2.8. Identification of antifungal VOCs using SPME-GC/MS

The identification of the antifungal VOCs produced by the three bacterial strains with strongest effect against Fmed, was performed using SPME GC-MS.

Briefly, a 1-week culture of Fmed Ph CO 36 on malt agar was placed onto one base of TSA plate on which 100 µL of a fresh bacterial suspension with a concentration of 10^9 CFU/mL was inoculated (one strain per condition), the two plates were sealed using parafilm and then incubated at 28 °C for seven days. Cultures of Fmed or bacteria and an uninoculated medium were used as control. Three biological replicates were performed per condition.

The VOCs were extracted using the SPME fiber 50/30 µm DVB/CAR/PDMS, 24 Ga, Manual Holder, 3 pk (Supelco, Sigma-Aldrich, US) that was carefully inserted in the headspace between the two petri plates. The fiber was placed in between the two plates during 30 min at 28 °C, to extract the microbial volatile metabolites. The analytes were desorbed for 5 min at 240 °C in the GC injector, the injection is carried out in splitless mode at 240 °C in the GC injector. A gas chromatograph Clarus 680 (Perkin-Elmer, USA) coupled with a MS detector (Perkin-Elmer, USA) was used to analyze the volatile compounds. The separation of the volatile compounds was achieved on the capillary column, ELITE-5MS 60 m × 0.25 mmID, 0.25 µm df (Perkin-Elmer, USA), Helium 6.0 (Air Liquide, France) was used as carrier gas with a constant flow rate of 1 mL/min. The oven temperature was initially held at 40 °C for 4 min, followed by a first temperature rise to 200 °C at a rate of 5 °C/min, then a second temperature rise to 250 °C at a rate of 20 °C/min. The total time of analysis was 34 min 50 s. Acquisition was carried out in scan mode with mass ranging from 35 to 350 *m/z* and identified using the library NIST (National Institute of Standards and Technology, v2.4–2020).

2.8.1. In vitro antifungal activity of selected individual VOC

The major metabolite produced by the two bacterial strains which

demonstrated the strongest inhibitory activity against Fmed in the indirect confrontation assay was selected to investigate whether this metabolite can inhibit Fmed growth in its pure form.

Briefly, four cultures of Fmed Ph CO 36 of seven days were placed in a sealed box, 20 ppm of the pure metabolite were injected in the air-tight box, the setup was incubated seven days at 28 °C. An uninjected set-up with four Fmed cultures of seven days was used as control. The percentage of Fmed growth inhibition was assessed by measuring the radius of the colonies in mm after seven days.

2.9. Identification of the extracellular bacterial metabolites using LC-MS/MS

The characterization of extracellular metabolites produced by the selected bacteria was investigated using LC-MS/MS.

To identify the extracellular metabolites produced by the bacteria, we cultivated Fmed Ph CO 36 in 15 mL of malt extract for seven days at 28 °C and 200 rpm, by the day seven, 100 µL of the bacterial suspension with a concentration of 10^9 CFU/mL was added, then incubated seven days at 28 °C, 200 rpm. Seven days later, the tubes were centrifugated 10 min at 5000 rpm, the obtained supernatant was filtered through 0.22 µm sterile Millex® syringe-driven filters (Merck Millipore). A cut-off at 2000 Da was performed using Vivacon® 500, 2000 MWCO HY filter, the collected filtrate was used for the characterization of the metabolite by LC-MS/MS. Cultures of Fmed or bacteria and an uninoculated medium were used as control, four biological replicates were prepared for each condition.

The chromatographic system used was an ultimate 3000 RSLC system (ThermoFisher Scientific, Germany), coupled with the MS detector Orbitrap Fusion Lumos high-resolution mass spectrometer (ThermoFisher Scientific, USA). The LC parameters were as follows: Column ACQUITY UPLC BEH C18 130 A 1,7 µm 2,1 × 100 mm (WATERS). Flow rate 0.4 mL/min, the column temperature was 45 °C. Mobile phase A was 0.1 % formic acid in water, mobile phase B was 0.1 % formic acid in acetonitrile. The LC separation was carried out with the following gradient: 0–1 min, 5 % B; 1–13 min, 5–95 % B; 13–15 min, 95 % B; 15–18 min, 5 % B. The AcquireX data acquisition workflow was used in deep scan mode. The sample injection volume was 10 µL per injection, with a total of four injections per sample. The first injection was used to perform a full MS scan and create a list of inclusion references. The subsequent three injections were used for the fragmentation of the *m/z* peaks that were added in the inclusion reference list (MS2). The FullMS resolution was set to 120000, and MS2 scans resolution set to 15000.

Data processing was carried out using Compound Discoverer 3.3 SP2 software (ThermoFisher Scientific, Waltham, MA). The annotation of the putative antifungal compounds was performed by comparing their calculated elemental composition with a manual constructed library of compounds reported in the literature for each strain. ChemSpider database was also used for the annotation of the detected metabolites. The function Fragment Ion Search (FISh) scoring algorithm was used to calculate the matching score by comparing the predicted fragment ions with the observed fragment ions. The data analysis was performed after the exclusion of the molecules identified in the cultural medium. A more detailed analysis was performed by focusing exclusively on molecules that are overexpressed in the coculture condition of Fmed with the biocontrol bacteria (ratio $\geq$ 1.2), while excluding metabolites from Fmed. Based on scientific literature on antifungal compounds from *Pseudomonas* and *Paenibacillus*, we compiled a mass list of these antifungal compounds and incorporated them into Compound Discoverer for targeted analysis.

2.10. Statistical analyses

Statistical analyses were performed using the R statistical software (version R4.2.1). Data obtained from microcosm assays were compared using an analysis of variance (ANOVA) Pairwise comparisons, were performed using Tukey's test ($p < 0.05$). PCoA were performed using the FactoMineR and factoextra packages.

3. Results

3.1. In vitro degradation of wood compounds

The 58 bacterial strains isolated from grapevines wood and sap were assessed for their *in vitro* ability to metabolize the three main components of wood, i.e., cellulose, hemicellulose (xylan) and lignin.

None of the bacterial isolates was able to degrade the Remazol Brilliant Blue R (RBBR) dye, suggesting the absence of ligninolytic activity *in vitro* (Table S1). In addition to the absence of ligninolytic activity, 14 bacterial isolates among the 33 isolates obtained from wood and nine isolates from sap were unable to degrade cellulose and xylan (Table S1), suggesting the absence of cellulolytic and xylanolytic activity *in vitro*. Seventeen strains obtained from wood and 13 from sap have shown moderate cellulolytic activity, while one strain obtained from sap (*Bacillus* sp. SV57) has shown a high cellulolytic activity. Two strains isolated from wood and three from sap have shown a moderate degradation of cellulose and xylan. This indicates that, overall bacterial strains either from wood or sap have similar degradative abilities.

3.2. In vitro activity of bacterial grapevine isolated against Fmed

The antagonistic activity of the 58 bacterial strains was evaluated *in vitro* against Fmed strain Ph CO36. We used two methods: (i) direct confrontation (DC) with bacterial production of diffusible metabolites coming into direct contact with the fungus and (ii) indirect confrontation by bacterial production of volatile organic compounds (VOCs) without any direct contact between the bacterial colonies and Fmed.

For the 33 bacteria isolated from the wood, in direct confrontation assay, three strains *Bacillus* sp. S147, *Pseudomonas paracarnis* S45 and *Stenotrophomonas* sp. S101 have shown more than 50 % of radial growth inhibition after one week of coculture with Fmed (Fig. 1). The highest percentage of Fmed growth inhibition was obtained with *Pseudomonas paracarnis* S45 (56 %). The other 29 strains have inhibited Fmed growth by less than 40 % (Fig. 1).

After one week of exposure to VOCs, 29 out of 33 strains isolated from wood inhibited Fmed growth by more than 50 % and 22 strains inhibited Fmed growth by more than 80 % (Fig. 1).

In the direct confrontation assay, four strains out of the 25 isolated from sap were able to inhibit Fmed growth by more than 60 % (Fig. 2) with 67–82 % of inhibition for three *Paenibacillus* strains SV20 (82 %); SV13 (78 %), SV23 (67 %) and with 64 % of inhibition for one *Bacillus* strain. For the volatile organic compounds assay, 20 strains out of the 25 isolated from sap inhibited Fmed growth by more than 50 %. Only five strains have inhibited Fmed growth by more than 80 %. Strikingly, the most effective bacterial strains in direct confrontation (*Paenibacillus* sp. SV23, SV20, and *Paenibacillus polymyxa* SV13) have shown the lowest percentage of Fmed growth inhibition in VOCs (Fig. 2).

3.3. Conservation of antagonistic capacities on diverse Fmed strains

In direct confrontation assays, the *Paenibacillus* sp. strains SV20, SV23, SV13, *Bacillus* sp. strains SV57 and S147, and *P. paracarnis* S45 were the most effective against all the tested Fmed isolates, inhibiting Fmed growth by over 40 % (Fig. 3). Among the 10 bacteria isolated from sap, eight inhibited the growth of nearly all the Fmed isolates. Although the strains *Bacillus* sp. S186 and *Luteibacter* sp. S167 were highly effective against Ph CO 36 in direct confrontation, they were less effective against the other five Fmed strains. In the VOCs assay, most bacterial strains effectively inhibited all Fmed isolates, with *Bacillus* sp. S186, *Bacillus* sp. S147, *Stenotrophomonas* sp. S101, and *P. paracarnis* S45 being the most effective (Fig. 3). Notably, *Paenibacillus* strains SV13, SV20, and SV23, which excelled in direct confrontation, exhibited the lowest

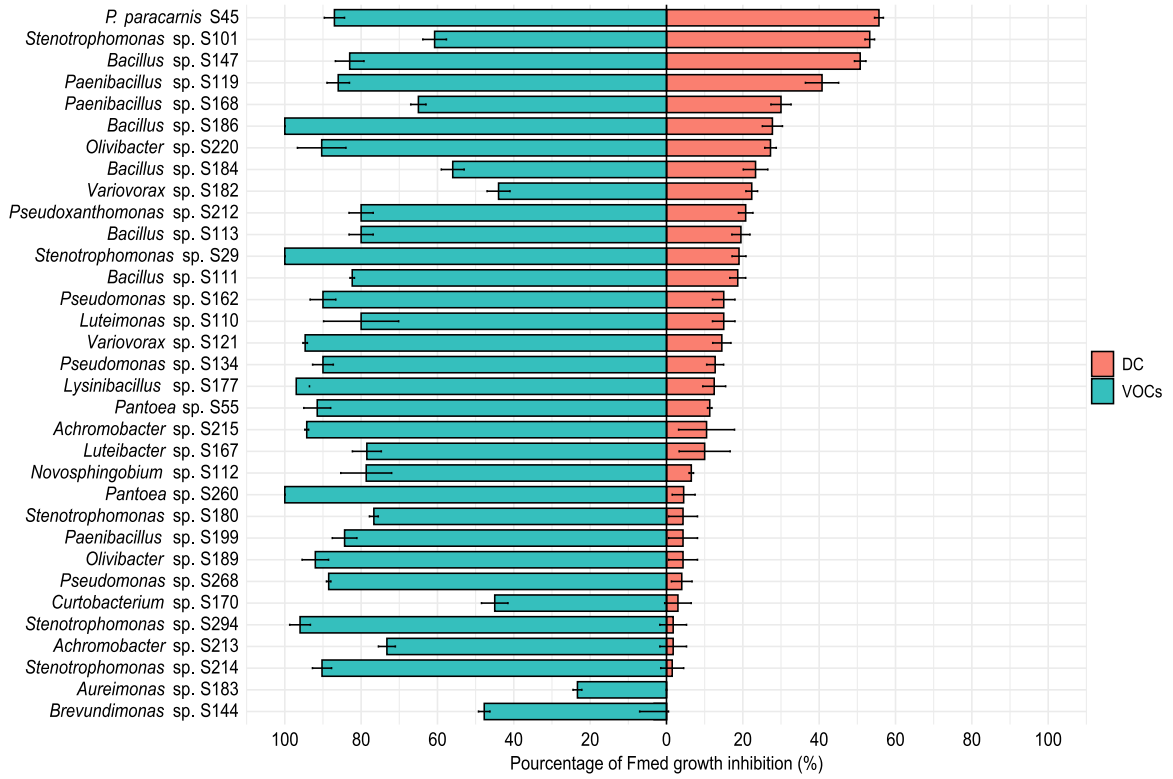

Fig. 1. *In vitro* growth inhibition of *Fomitiporia mediterranea* Ph CO 36 by bacteria isolated from grapevine wood tissues through direct confrontation (DC) and volatile organic compounds (VOCs).

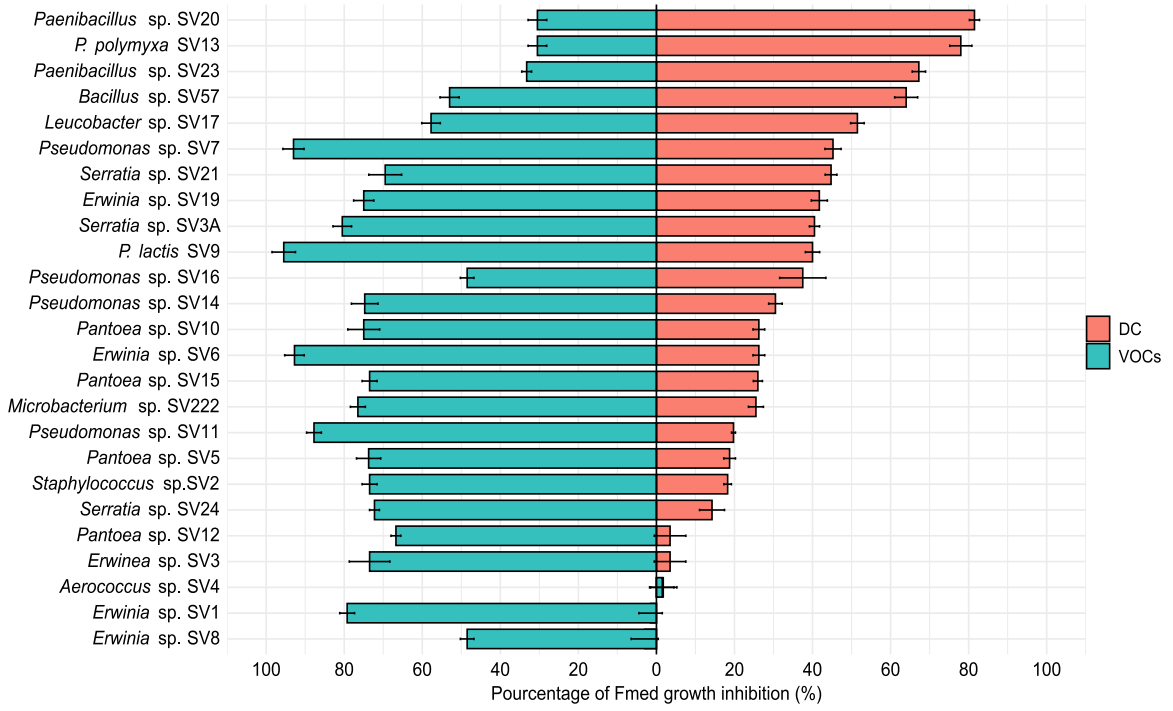

Fig. 2. *In vitro* growth inhibition of *Fomitiporia mediterranea* Ph CO 36 by bacteria isolated from grapevine sap through direct confrontation (DC) and volatile organic compounds (VOCs).

inhibition rates in the VOCs assay (Fig. 3).

We selected the 10 strains (S101, S147, S186, S45, SV13, SV20, SV23, SV57, SV7 and SV9) that showed the strongest inhibition of Fmed growth *in vitro* for our further studies.

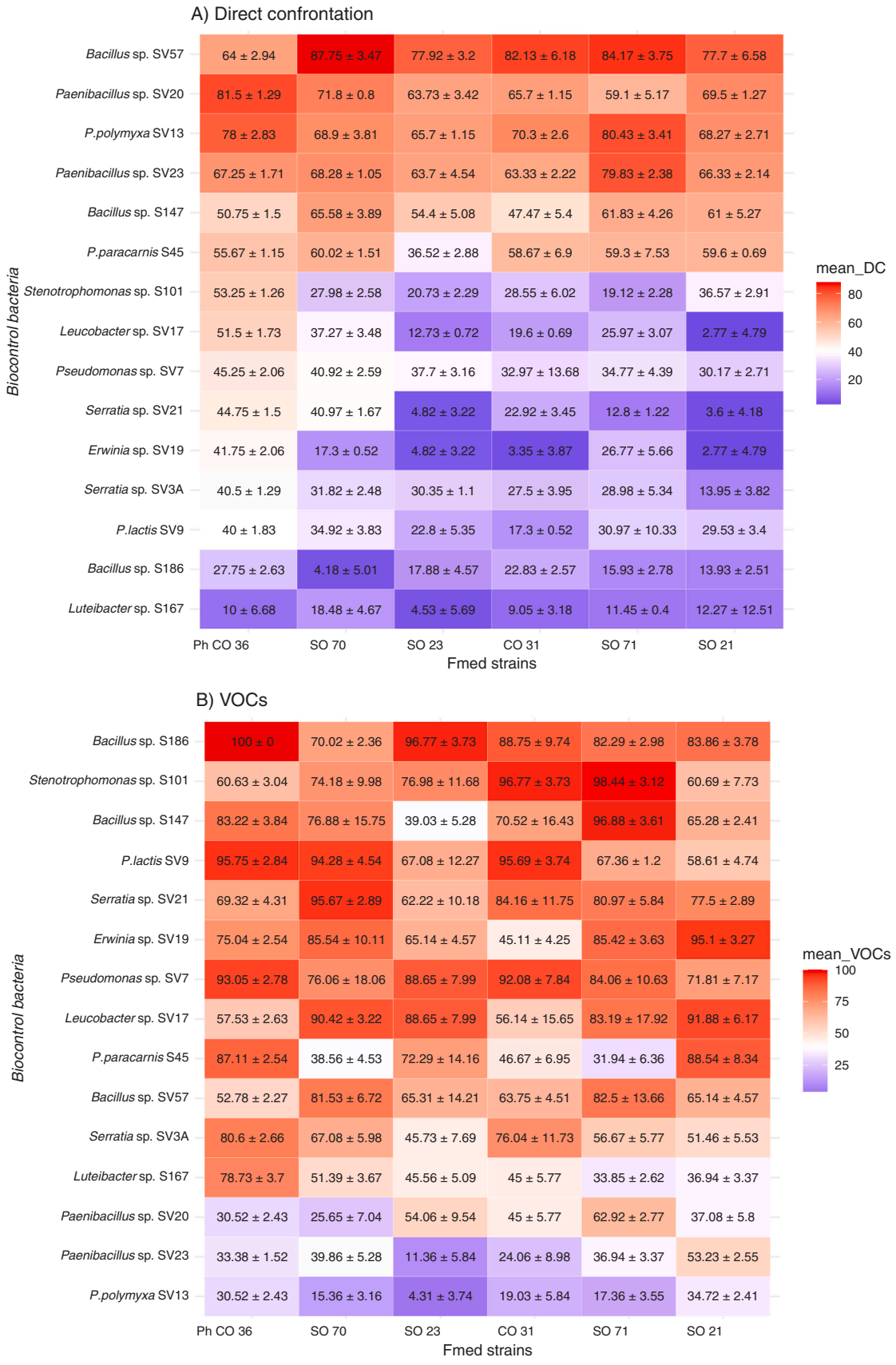

Fig. 3. Growth inhibition of six *Fomitiporia mediterranea* strains *in vitro* by bacteria isolated from grapevine sap and wood: A) Direct Confrontation and B) VOCs.

3.4. Confrontation assays in grapevine sawdust microcosms

In order to assess the efficiency of bacteria in more realistic conditions we determined their ability to limit Fmed Ph CO 36 growth on pruning wood and healthy trunk wood sawdust of the cultivar Ugni Blanc. Using a curative method, where the bacteria were inoculated seven days after Fmed inoculation on sawdust, simulating the conditions of a curative solution in vineyards, where biocontrol agents are introduced into diseased plants. Here, we present only the results obtained on the trunk wood sawdust, as similar findings were observed for the pruning wood sawdust.

Among the 10 bacterial strains tested only three; *P. paracarnis* S45, *P. lactis* SV9 and *P. polymyxa* SV13 have inhibited Fmed growth on the Ugni Blanc wood sawdust. The two strains isolated from sap, *P. lactis* SV9 and *P. polymyxa* SV13, have totally inhibited Fmed growth immediately and durably over the three weeks (Fig. 4). The strain *P. paracarnis* S45 isolated from wood inhibited the radius growth of Fmed by 33 % by day seven and 14 and was not observed by 21 days (Fig. 4). However, the mycelium density of Fmed after inoculation with this bacterial strain was reduced by 80 % by the day seven and 14. After 21 days of *P. paracarnis* S45 inoculation, the Fmed mycelium density was reduced by 71.8 % (Fig. 4). The seven remaining bacterial strains exhibited weak inhibition of Fmed growth in the microcosm assay, which was inconsistent with the strong inhibition percentages recorded in the direct and indirect confrontation assays, where these strains had demonstrated a strong capacity to inhibit Fmed growth (Figs. 1 and 2 vs Fig. 4).

While *Paenibacillus* sp. SV20 and SV23 showed the highest inhibition of Fmed in *in vitro* assays they had the lowest efficacy in the sawdust microcosm. Therefore, we selected *P. polymyxa* SV13, *P. lactis* SV9, and *P. paracarnis* S45 for further analyses due to their consistent and high efficacy in both *in vitro* and sawdust microcosm conditions where they significantly reduced Fmed radial growth and mycelium density.

3.4.1. Conservation of antagonistic capacities in sawdust microcosm from different grapevine cultivars

To investigate whether the three bacterial strains selected on microcosm of Ugni Blanc cultivar, were also efficient against Fmed if grown on other grapevine cultivars, we assessed the antagonistic activities on six additional cultivars i.e., Baroque (BRQ), Cabernet Franc (CF), Cabernet sauvignon (CS), Gros Manseng, (GM), Fer Servadou (FS) and Sauvignon Blanc (SB). The three bacterial strains were evaluated for their abilities to inhibit Fmed growth, called here “curative application”, or to prevent the wood colonization by Fmed, called here “preventive application”.

Compared to the results obtained on Ugni Blanc, the percentage of the radial growth inhibition of Fmed for the three selected bacterial strains was lower on the six other cultivars and varied from very strong to weak inhibition depending on the bacterial strains and grapevine cultivar (Fig. 5).

Overall, *P. paracarnis* S45 and *P. lactis* SV9 decreased the mycelial density of Fmed on all grapevine cultivars by more than 36 % (except on the cultivar Cabernet Sauvignon) but this was not linked to a strong Fmed radial growth inhibition. Similarly, *P. polymyxa* SV13 decreased the mycelial density of Fmed by more than 40 % on five out of the seven grapevine cultivars and weakly inhibited Fmed radial growth. We observed the same trends after 14 and 21 days of coculture (data not shown).

When applied preventively, all three bacterial strains inhibited Fmed growth strongly on sawdust from Baroque and Ugni Blanc cultivars. For the other cultivars, the three strains inhibited Fmed growth only weakly (Fig. 6).

We observed similar trends for both measurements after 14 and 21 days of coculture with the bacteria at each time (data not shown).

3.5. Genomes of the bacterial strains P. paracarnis S45, P. lactis SV9, and P. polymyxa SV13

The genomes of the biocontrol strains *P. paracarnis* S45, *P. lactis* SV9, and *P. polymyxa* SV13 were analyzed to identify gene clusters associated with their biocontrol activities. Their genome sizes are 5.7, 6.2, and 5.1 Mb, respectively. The G+C content is similar for the *Pseudomonas* strains (60.3 % for S45 and 60.1 % for SV9), while the *Paenibacillus* strain has a lower content of G+C (45.8 %). The number of predicted coding sequences (CDSs) is 5069 for S45, 5527 for SV9, and 4557 for SV13. Key genomic features are summarized in Table 1.

The functional gene annotation was carried out using multiple general databases. RAST annotation allowed the detection of genes encoding different functions (Table S2.a, S2.b and S2.c). The distribution of genes into COG functional categories is presented in Fig. 7and Figure S1. The genomes of the *Pseudomonas* strains harbor mainly genes involved amino acids/derivatives metabolization (~20 %), followed by genes involved in carbohydrate metabolization (~10 %). In contrast, the genome of *P. polymyxa* SV13 contains primarily genes related to carbohydrate metabolism (19.6 %), followed by those involved in the metabolism of amino acids and their derivatives (16.7 %). (Figure S1). AMR genes were screened by mapping the filtered reads from the whole genome sequencing to the Comprehensive Antibiotic Resistance Database (CARD). AMR genes were identified in the genomes of the three strains, with 14 genes detected in the genome of the strain S45, 15 genes were identified in the strain SV9, and two genes for the strain SV13 (Table S3.a, S3.b and S3.c).

Prediction of secondary metabolite biosynthesis gene clusters was

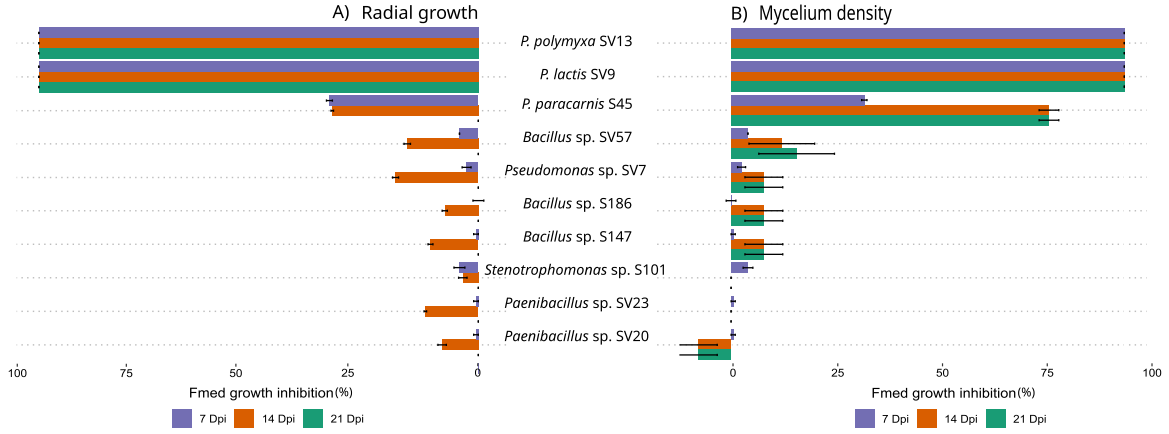

Fig. 4. A) Percentage of the radial growth inhibition and B) Percentage of the reduction of the mycelium density of *Fomitiporia mediterranea* Ph CO 36 on sawdust microcosm after bacterial inoculation. Dpi: days post-inoculation.

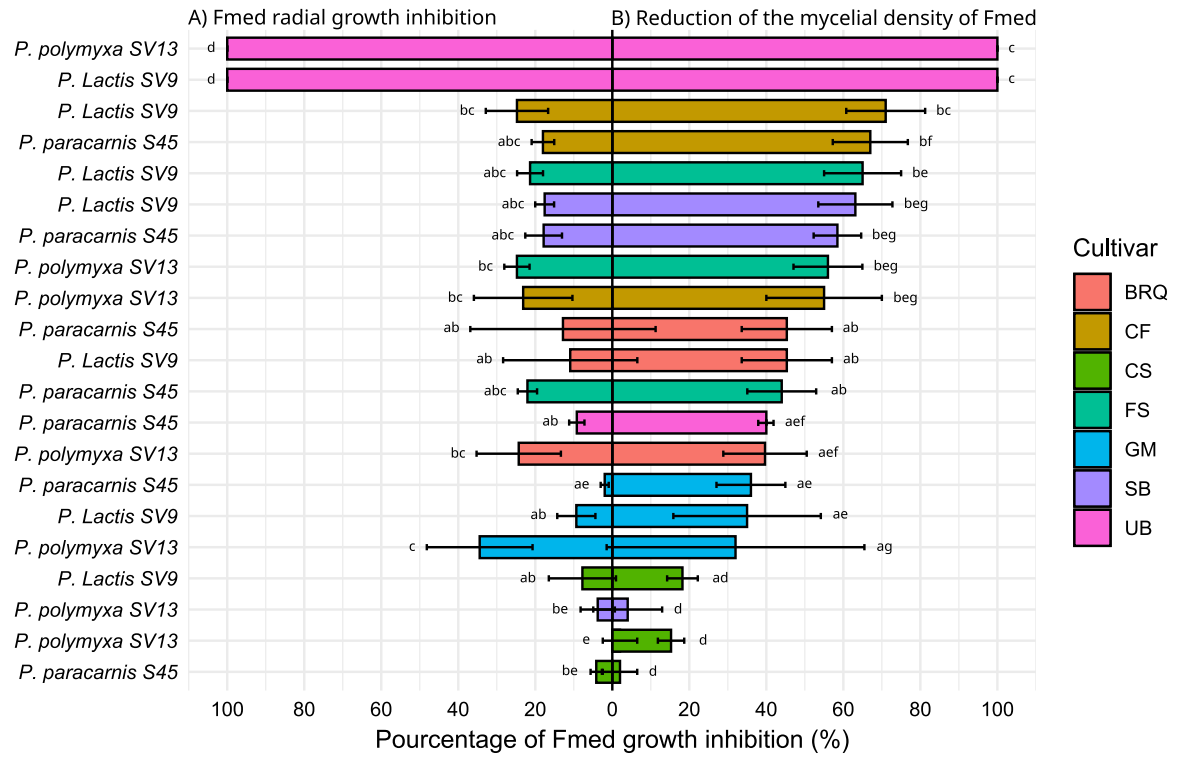

Fig. 5. Percentage of radial growth inhibition (A) and reduction in mycelium density (B) of *Fomitiporia mediterranea* Ph CO 36 on sawdust microcosm of seven grapevine cultivars, resulting from curative bacterial application i.e., at seven days after inoculation of the bacterial strains on the plate inoculated with *Fomitiporia mediterranea* grown previously for seven days. Separately for (A) and (B) in each panel, bars followed by different letters are significantly different ($p < 0.05$; Tukey test).

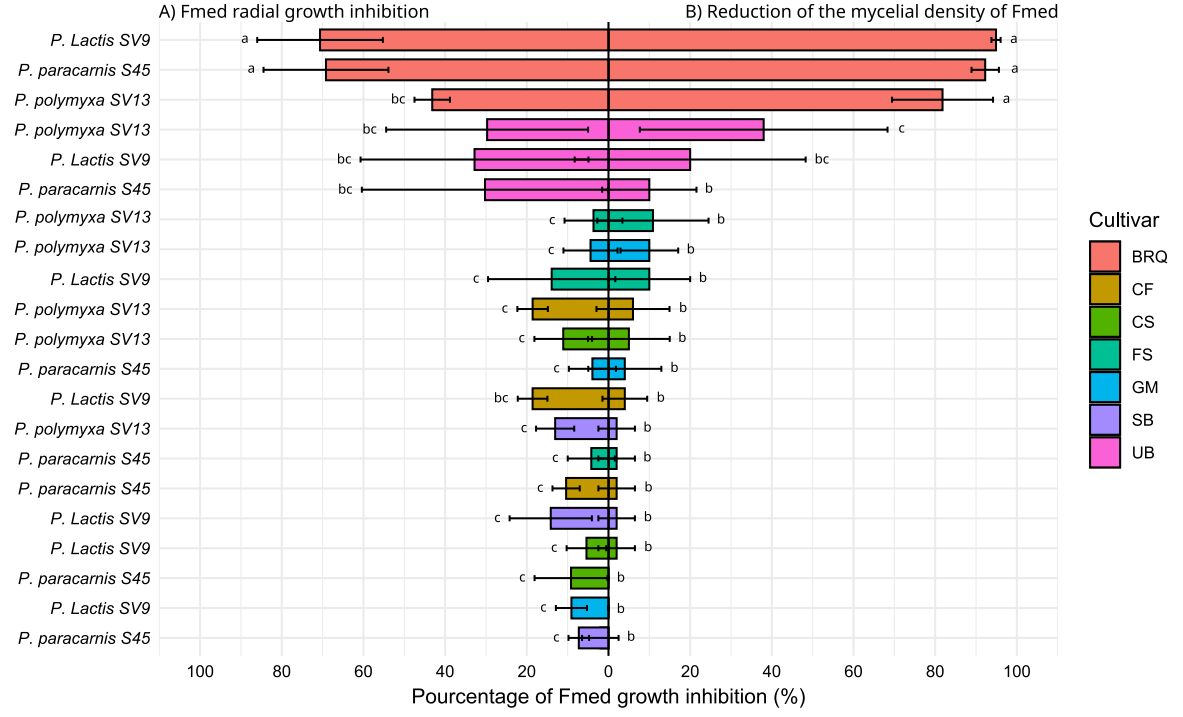

Fig. 6. Percentage of radial growth inhibition (A) and reduction in mycelium density (B) of *Fomitiporia mediterranea* Ph CO 36 on sawdust microcosm of seven grapevine cultivars, resulting from preventive bacterial application i.e., first an inoculation of the bacterial strains and three days later *Fomitiporia mediterranea* inoculation. Separately for (A) and (B) in each panel, bars followed by different letters are significantly different ($p < 0.05$; Tukey test).

Table 1
Summary of the features of the three strains: *Pseudomonas paracarnis* S45, *Pseudomonas lactis* SV9 and *Paenibacillus polymyxa* SV13.

Feature	S45	SV9	SV13
Sequence size (bp)	5708428	6272110	5198206
Number of contigs	26	32	54
GC content (%)	60.3	60.1	45.8
Coverage	753.3	571	704.7
Completeness (%)	99.8	99.74	99.85
tRNAs	62	63	96
tmRNAs	1	1	1
rRNAs	6	7	13
ncRNA regions	52	101	46
CRISPR arrays	0	0	1
CDSs	5069	5527	4557

performed using antiSMASH. The majority of them are antifungal metabolites, the others are siderophores, antibacterial and molecules involved in different signaling pathways (Fig. 7 and Figure S1).

The CAZyme profiles of the two *Pseudomonas* strains were similar (Fig. 8) with *P. paracarnis* S45 with genes encoding a total of 85 different CAZymes and *P. lactis* SV9 encoding 89 different CAZymes. These enzymes belong to six CAZymes classes and are distributed into 38 CAZymes families for the strain S45, and into 40 families for the strain SV9. Genes of the *Pseudomonas* strains encode mainly Glycosyl Hydrolase (GH) and Glycosyl Transferases (GT) enzymes (Table S4). We further detected in strain S45 32 GH and 33 GT related genes, while 35 GH and 35 GT in strain SV9. The CAZyme profile of *P. polymyxa* SV13 was different compared to the one of the *Pseudomonas* strains. We found 262 different CAZyme-related genes in *P. polymyxa* SV13 that belong to seven CAZymes classes and are distributed into 96 CAZymes families, 130 of them are GH and 58 are GT. Unlike the *Pseudomonas* strains, genome prediction shows that *P. polymyxa* SV13 encodes a S-layer homology domain (SLH), which is critical for forming cellulosomes, a multi-protein complex that can efficiently degrade carbohydrate-rich biomasses (Fig. 8). The most abundant CAZyme family for the three bacterial strains is GT2, followed by GT4 for the strain SV13 (Table S4).

3.6. Plant growth-promoting traits

By mapping the bacterial coding sequences to the Plant-associated Bacteria Database from PLaBAse, we investigated the potential of the three bacterial strains to act as plant growth-promoting bacteria (PGPB). This analysis enabled us to identify the functional genes involved in both direct and indirect plant growth-promotion mechanisms (Fig. 9). Most identified gene categories are involved in the regulation of indirect mechanisms of plant growth promotion. Among these, the genes encoding for plant system colonization were the most abundant across all three strains, followed by those involved in regulating competitive exclusion, stress control, and plant response stimulation. For direct mechanisms, the most abundant genes are those encoding proteins linked to biofertilization, along with others responsible for regulating phytohormone production and bioremediation (Fig. 9).

The genome of the three bacterial strains further harbor PGPTs which regulate several important functions of biocontrol agents, such as the neutralization of biotic and abiotic stress, heavy metal detoxification, phosphate solubilization, iron acquisition, nitrogen acquisition, the induction of the systemic resistance (IRS), the production of phytohormones and the resistance to plant antimicrobial metabolites (Table 2).

Among the PGPTs that are involved in the neutralization of the biotic stress found in the genomes of the three strains, we identified genes encoding for fungicidal compounds, some of theme encode chitinases, that may degrade the fungal cell-wall, others encode antifungal metabolites. The strain *P. polymyxa* SV13 encodes fusaricidin which is an antifungal metabolite. Regarding the neutralization of abiotic stress, the three genomes harbor genes involved in the tolerance towards high and low temperatures. Among the genes involved in iron acquisition pathways, we identified a gene encoding pseudomonine.

3.7. Prediction of secondary metabolite biosynthesis gene clusters

Secondary metabolite biosynthesis gene clusters in *P. lactis* SV9, *P. Paracarnis* S45, and *P. polymyxa* SV13 were determined using antiSMASH. In both *Pseudomonas* genomes, a total of 16 potential gene clusters involved in secondary metabolite production were identified, and 21 for *P. polymyxa* SV13 (Table 3).

For *P. paracarnis* S45 a gene cluster encoding a siderophore with 100 % of similarity to pseudomonine was identified. Another cluster encoding for arylpolyene with 40 % similarity to APE Vf. The remaining 14 clusters found encode for siderophores, betalactones, NRPS (Non-ribosomal peptide synthetase), NRPS-like and redox cofactors but display low similarity to known clusters. Two clusters with 25 % and 13 % of similarity to fragin and fengycin respectively were identified (Table 3).

In *P. lactis* SV9 a related NRPS showed 100 % similarity to most similar known cluster related to rhizomide. A cluster with 45 % similarity to arylpolyene, APE Vf was also identified in SV9 genome. As for *P. paracarnis* S45, two clusters with similarities to fragin and fengycin cluster genes were identified in SV9 and one cluster was assigned to the antimicrobial NRPS viscosin (Table 3).

Three clusters among the 21 identified in *P. polymyxa* SV13 showed 100 % similarity to known clusters genes, one encodes the lanthipeptide paenilan and two encode the antifungal NRPS, polymyxin and fusaricidin. Two clusters had 80 % and 40 % of similarity with tridecaptin cluster genes and one had 63 of similarity to paenithipeptin synthetic genes. A cluster was assigned to genes encoding the antifungal lasopeptide paeninodin (40 %) (Table 3).

3.8. Identification of bacterial antifungal VOCs

The VOCs produced by the three bacterial strains, *P. paracarnis* S45, *P. lactis* SV9 and *P. polymyxa* SV13 when cultivated in pure culture or with Fmed for seven days, were identified using SPME-GC-MS.

The two *Pseudomonas* strains S45 and SV9 had a similar volatile footprint, very different from that of *P. polymyxa* SV13, characterized by a unique peak population. Only 10 VOCs were detected in the sample Fmed and the presence of Fmed did not affect significantly the volatolome of the three bacterial strains. The metabolomic profiles of the samples of bacteria grown in presence of Fmed were different from the profiles of the bacteria grown alone and more similar to the profile of Fmed grown alone. This is due to the high abundance of Fmed metabolites in the volatolome of samples of bacteria and Fmed grown together. (Fig. 10).

The most abundant metabolites produced by Fmed were M-8-Methylnonanoic acid-isopropyl ester, methyl 2-furoate, and benzoic acid methyl ester (Fig. 11). The concentrations of these metabolites declined in the presence of the bacterial strains. *P. polymyxa* SV13 produced mainly pyrazine, 2,3-dimethyl-5-(1-methylpropyl), both in pure culture and in the presence of Fmed. 2-(2-Methylpropyl)-3-(1-methylethyl) pyrazine is another metabolite containing the pyrazine group which was identified in the headspace of this strain. As for the *Pseudomonas* strains, the disulfide, dimethyl (DMDS) followed by 1-undecene were the most detected metabolites and did not decrease in the presence of Fmed (Fig. 11). The majority of VOCs that were identified in the cultures of the *Pseudomonas* strains were sulfur-containing compounds (DMDS, Methanethiol, dimethyl sulfide, methyl thioacetate) and alkanes.

We determined the concentration of DMDS in the headspace of the setup and demonstarted that the application of 20 ppm of DMDS to Fmed cultures reduced its growth by 15.2 % compared to the control.

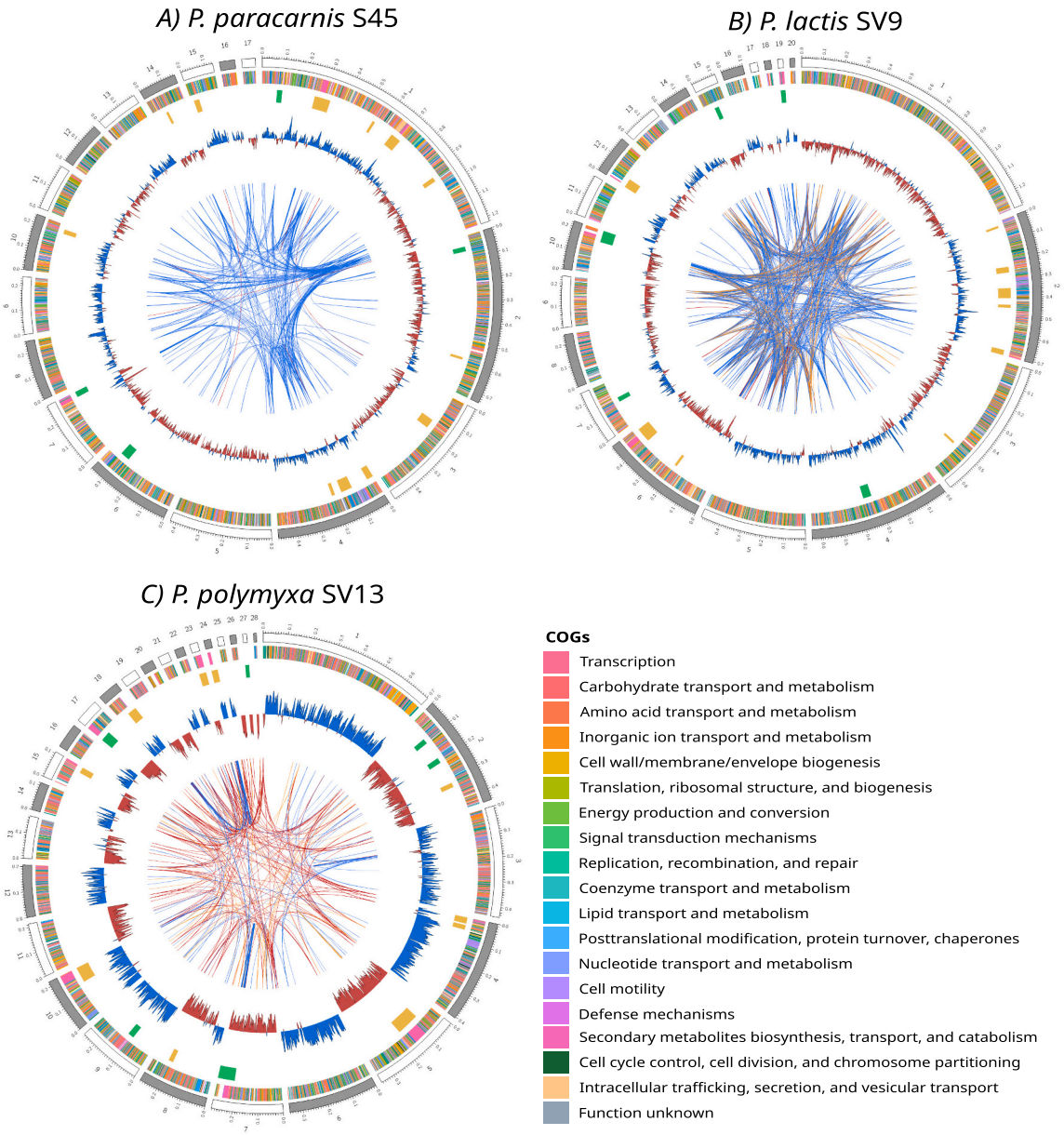

Fig. 7. Circular visualization of genomes using Circos, (A) *Pseudomonas paracarnis* S45; (B) *Pseudomonas lactis* SV9; (C) *Paenibacillus polymyxa* SV13. From outside to inside: 1st layer – Contigs in alternating white and grey color with tick marks every 10 kbp and labels every 100 kbp expressed in Mbp. The contigs are numbered in order of size. For the sake of visualization, only contigs with a size > = 10 kbp are represented. Ticks are only present on contigs with a size > = 100kbp. 2nd layer – COG affiliations of gene products. 3rd layer – Regions of secondary metabolism as identified by Antismash. Regions involved in the production of antifungal compounds are depicted in green, all other regions are depicted in yellow. 4th layer – GC skew diagram representing the local variations in GC content to the environing mean GC content. Above average values are depicted in blue and below average values in red. GC content variations were calculated in a 5 kb sliding window with a 1 kb step size. 5th layer – Genomic region similarities. Regions with a similarity level > 95 % are depicted in red, > 90 % in orange and > 70 % in blue.

3.9. Identification of the extracellular bacterial antifungal metabolites

As shown in Fig. 12, the metabolome of *P. polymyxa* SV13 differed significantly from that of the two *Pseudomonas* strains. The presence of Fmed induced an important modification in the metabolome of SV13. The metabolomes of the two *Pseudomonas* strains, S45 and SV9 were highly similar and the presence of Fmed which induced a slight modification in there metabolomic profile. The metabolomic profiles of the samples of *P. paracarnis* S45 and *P. lactis* SV9 grown in presence of Fmed were different from the profiles of each of the bacteria grown alone and similar to the profiles of Fmed grown alone. This shows the high abundance of Fmed metabolites in the metabolome of samples where bacteria and Fmed were grown together (Fig. 12).

We identified the bacterial antifungal metabolites for each strain, focusing exclusively on those that are overexpressed when cocultured with Fmed, and excluding Fmed's metabolites (Fig. 13, Table S5). *P. polymyxa* SV13 produced Xenocoumacin 1, fusaricidin type compounds (A, A1, B, C, D and 1032) and indole-1-Benzanole, all known as antifungal compounds (Fig. 13). *P. paracarnis* S45 and *P. lactis* SV9 produced bacilysin and vazabitide, known as antifungal metabolites, in addition to the quorum sensing signal molecule N-Butyryl-L-homoserine lactone; all were overexpressed in the presence of Fmed. The siderophore pseudomonine was also detected in the metabolome of the three strains.

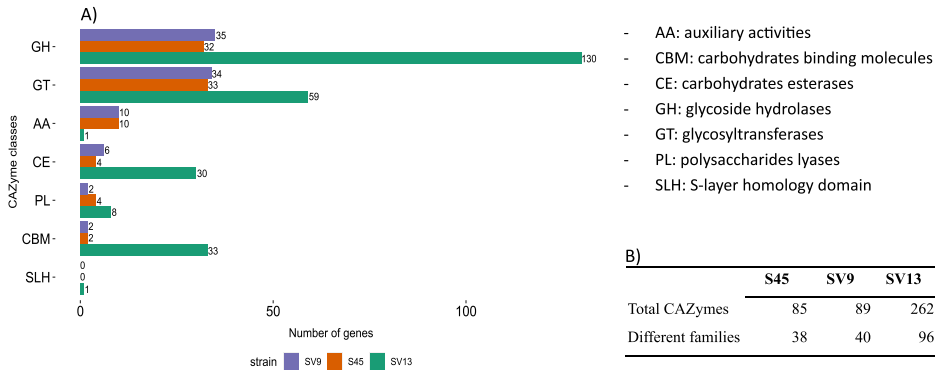

B)

	S45	SV9	SV13
Total CAZymes	85	89	262
Different families	38	40	96

Fig. 8. (A) Carbohydrate-active enzymes (CAZymes) related genes of the strain *Pseudomonas lactis* SV9, *Pseudomonas paracarnis* S45 and *Paenibacillus polymyxa* SV13. (B) Total CAZymes and different families for each bacterial strain.

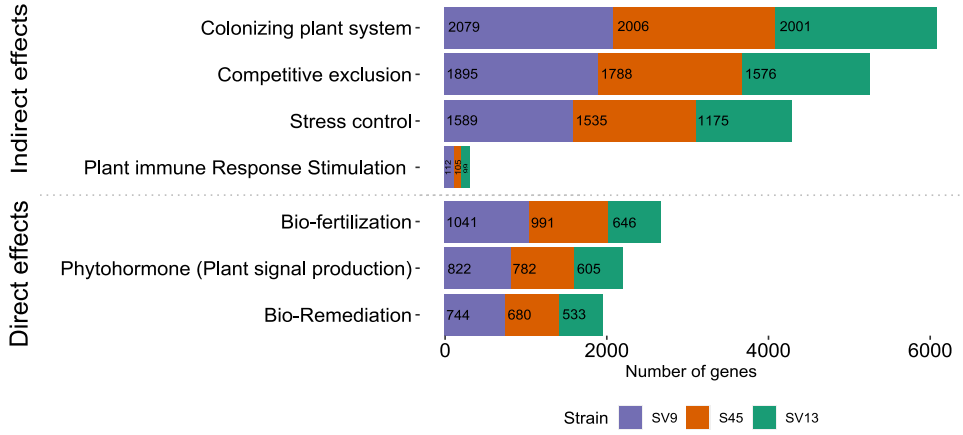

Fig. 9. Plant growth-promoting traits groups identified in *Pseudomonas paracarnis* S45, *Pseudomonas lactis* SV9 and *Paenibacillus polymyxa* SV13.

4. Discussion

In this study we examined the antagonistic activity of 58 bacteria isolated from grapevine wood or sap against Fmed, one of the most important pathogens associated with Esca. We selected the three most effective bacterial strains against Fmed in sawdust microcosms, and used both genomic and metabolomic approaches to decipher their mechanisms of action.

To be used as biocontrol bacteria without harming grapevine wood, the selected strains were first tested for their ability to degrade plant wood components such as lignin, cellulose and hemicellulose. We have shown that none of the three bacterial strains exhibited a ligninolytic activity *in vitro*, which is consistent with previous studies by Hervé et al., (2016) and Haidar et al., (2021). We also found that most of the tested strains do not exhibit cellulolytic and xylanolytic activities *in vitro*, which aligns with the results reported by Haidar et al. (2021). Lignin is a phenolic polymer that is cross-linked with cellulose and hemicellulose, which makes it challenging for microorganisms to access (Cragg et al., 2015). It was reported that the degradation of the plant cell wall is a complex enzymatic process and the access to the cell wall carbohydrates requires lignin bypass or degradation (Cragg et al., 2015). We thus suggest that the inability of the bacterial strains used in this study to degrade lignin limits their access to cellulose and hemicellulose in plant cell walls. This characteristic makes them suitable for use as biocontrol bacteria.

In our experiment, 51 out of 58 strains exhibited strong inhibition of Fmed growth through their VOCs, which is consistent to previous results by Haidar et al. (2021) on the same pathogen. Our observations indicate that bacteria highly effective in inhibiting Fmed growth through VOCs production were generally less effective in direct confrontation, and conversely, strains that were highly effective in direct confrontation were less effective through VOCs production. This suggests that bacterial strains may inhibit pathogens via VOCs, diffusible metabolites, or both, but not necessarily with equal efficiency. Fmed growth inhibition was observed when bacteria are present and in favorable conditions to metabolites production. Our results don't give clues about the duration of the inhibition in case of cessation of bacterial metabolite production. The mode of action thus needs to be considered when selecting BCAs to be used in real conditions.

Fmed growth inhibition depended on the sampling site of bacteria in the grapevine, i.e., either wood or sap. The diffusible bacterial metabolites in the direct confrontation assays caused moderate to weak inhibition of Fmed growth when they were produced by wood-colonizing bacteria, while roughly all strains isolated from sap moderately to strongly inhibited Fmed by their agar-diffusible metabolites. Moreover, bacteria isolated from healthy wood tissue have shown stronger antifungal activity against Fmed compared to those obtained from necrotic tissue, which aligns with the findings of Haidar et al. (2021). Here, this result is likely due to differences in the bacterial communities of the grapevines, influenced by their disease state. Whereas, wood-associated bacteria were isolated from grapevines expressing severe Esca symptoms, sap-associated bacteria were isolated from plants with either mild or no Esca symptoms. Therefore, considering this criterion when selecting a biocontrol agent would be worthwhile.

Overall, we have shown that the 15 bacterial strains able to inhibit the growth of the strain Ph CO 36, also inhibited the growth of five alternative Fmed strains. However, we showed a stronger inhibitory effect against Fmed Ph CO 36 comparing to the five other strains of

Table 2
Plant growth-promoting traits identified in *Pseudomonas paracarnis* S45, *Pseudomonas lactis* SV9 and *Paenibacillus polymyxa* SV13.

PGPTs group		PGPTs category	Number of genes		
			S45	SV9	SV13
Direct effects	Bio-fertilization	Nitrogen Acquisition	162	176	89
		Carbon Dioxide Fixation	22	22	22
		Phosphate Solubilization	282	293	200
		Potassium Solubilization	235	239	143
		Sulfur Assimilation/Mineralization	72	75	34
		Iron Acquisition	218	236	158
	Bio-remediation	Heavy Metal Detoxification	447	469	366
		Xenobiotics Biodegradation	232	274	167
	Phytohormone; plant signal production	Abscisic Acid Degradation	41	48	14
		Jasmonate Production	2	2	0
		Cytokinins/derivate Production	33	32	1
		Gibberellins Production	1	1	29
		Terpenoid/derivate Production	31	28	6
		Gamma-Aminobutyric Acid Production	26	32	14
		Plant Signal-Phospholipid Production	33	35	39
		Plant Signal-Branching Stimulation	40	47	35
		Plant Signal-Branching Inhibition	51	58	67
		Plant Signal-Germination Stimulation	96	97	35
		Plant Signal-Embryogenesis	51	58	82
		Plant Signaling Volatiles	121	133	226
		Plant Vitamin Production	239	235	15
		Plant Signal-Carnitine Production	1	0	0
		Plant Signal- Ubiquinone/Coenzyme Q Production	16	16	0
Indirect effects	Stress control; Biocontrol	Neutralizing Biotic Stress	301	320	273
		Neutralizing Abiotic Stress	1070	1087	734
		Universal Stress Response	164	182	168
	Plant immune response stimulation	Induction Of Systemic Resistance (ISR)	76	80	70
		Induction Of Systemic Acquired Resistance (SAR)	8	4	0
		Triggered Immunity	21	28	29
	Colonizing plant system	Motility; Chemotaxis	213	220	1424
		Plant Derived Substrate Usage	1377	1414	105
		Root Colonization	116	120	164
		Surface Attachment	167	185	142
		Plant Cell Wall/Membrane Degradation	36	39	32
		Adaption to Plant Immune System	69	71	20
		Other Colonization Related Proteins	28	30	284
	Competitive exclusion (CE)	Cell Envelope Remodeling	291	297	133
		Spore Production	7	7	374
		Quorum Sensing Response; Biofilm Formation	569	568	214
		Exopolysaccharide Production; EPS	134	134	498
		Bacterial Fitness	584	641	73
		Bacterial Secretion	203	248	0

Fmed. This efficiency, depending on pathogenic strain, was previously reported by Mondello et al., (2019). The authors demonstrated that the biocontrol strain *Fusarium proliferatum* was highly effective *in vitro* against *Neofusicoccum parvum* strain "Saint Victoire", but its effectiveness was reduced against two other strains of *N. parvum* under the same conditions. This illustrates one of the biases in selecting biocontrol agents performed with an efficiency screening against one pathogen, thus leading frequently to lower efficiency when the BCA is used on other pathogen strains. In the case of Fmed, this variability could be due to the production of specific compounds by biocontrol bacterial strains, such as narrow-spectrum antibiotics or enzymes that target particular components of the fungal cell wall or metabolic pathways present only in certain Fmed genotypes. In further studies, metabolic analyses using the same biocontrol strain against different Fmed strains could be useful in confirming this hypothesis.

The use of sawdust microcosms offers environmental conditions that are closer to grapevine wood, and improves the chance of positive correlations between our results and field efficacy (Köhl et al., 2020). In our study we observed a low correlation between the efficacy of the bacterial strains against Fmed *in vitro* on synthetic medium and on sawdust microcosms. Only three strains selected in the synthetic medium remained effective against Fmed when tested on grapevine sawdust of the cultivar Ugni Blanc that was used to select potential BCAs because of its sensitivity to Esca disease (Gastou et al., 2024). This clearly highlights that *in vitro* test of BCAs under more realistic conditions are crucial before field trials. We also demonstrated that Fmed inhibition on grapevine sawdust microcosms was strongly dependent on grapevine cultivars, with significant efficacy observed primarily in two cultivars: Ugni Blanc and Baroque. The variability related to cultivars may be explained by the differences in the chemical composition of the wood of each cultivar (Songy et al., 2019). As reported in the literature, the concentration of lignin and the vessels diameters may influence the grapevine sensitivity to Esca disease (Csótó et al., 2023; Pouzoulet et al., 2014; Rolshausen et al., 2008; Songy et al., 2019). For instance, Cabernet Franc, Cabernet Sauvignon, Sauvignon Blanc and Ugni Blanc have been identified as particularly sensitive to Esca (Martínez-Diz et al., 2020; Csótó et al. 2023; Gastou et al., 2024). One should note that our sawdust approach allows us to address differences in wood chemical composition but not variations in plant defenses and wood structures found in live plants. The choice of the application methods, i.e., curative or preventive significantly influenced the effectiveness of bacterial strains in inhibiting Fmed growth. Therefore, variations in the effectiveness of bacterial strains across different cultivars and application methods may be attributed to their capacity to grow on wood, as well as the specific characteristics of the wood from each cultivar, which can either facilitate or restrict bacterial colonization of the wood. Fungal activity and response to bacteria may also vary between cultivars and further impact bacterial efficacy. These factors should be thoroughly considered when assessing and selecting BCAs for effective disease management.

Understanding the mechanisms of action of biocontrol agents against

Table 3
The predicted secondary metabolite gene clusters in *Pseudomonas paracarnis* S45, *Pseudomonas lactis* SV9 and *Paenibacillus polymyxa* SV13 using antiSMASH (*metabolites detected In LC-MS/MS).

Type	Most Similar Known Cluster	Similarity		
		S45	SV9	SV13
Arylpolyene	Ape Vf	40 %	45 %	-
Betalactone	Fengycin	13 %	13 %	-
Lanthipeptide-Class-I	Paenilan	-	-	100 %
Lanthipeptide-Class-Iii	Paenithipeptin	-	-	63 %
Lassopeptide	Paeninodin	-	-	40 %
NI-Siderophore	Mevalagmapeptide A/ Mevalagmapeptide B/ Mevalagmapeptide C/ Mevalagmapeptide D	4 %	4 %	-
NRP-Metallophore, NRPS, Hydrogen-Cyanide	Pf−5 Pyoverdine	10 %	11 %	-
NRP-Metallophore, NRPS-Like,NRPS	Pseudomonine*	100 %	-	-
Nrps	Pf−5 Pyoverdine	10 %	10 %	-
	MA026	-	14 %	-
	Viscosin	-	43 %	-
	Rhizomide A/Rhizomide B/ Rhizomide C	-	100 %	-
	Polymyxin	-	-	100 %
	Fusaricidin B*	-	-	100 %
	Tridecaptin	-	-	40 %
	Tridecaptin	-	-	80 %
	Gramicidin S	-	-	6 %
	Thermoactinoamide A	-	-	100 %
NRPS-Like	Fragin	25 %	25 %	-
	Pyoverdine SMX−1	6 %	12 %	-
Redox-Cofactor	Lankacidin C	13 %	13 %	-
Ripp-Like	Lipopolysaccharide	5 %	5 %	-
	Lipopolysaccharide	-	-	-
Transat-PKS, NRPS, T3PKS, PKS-Like	Aurantinin B/Aurantinin C/ Aurantinin D	-	-	35 %

phytopathogens is essential to register them and to develop effective treatments for vineyard application. The most potent biocontrol agents are those that exhibit multiple mechanisms of action, targeting vital components and metabolic pathways of the pathogen. In this study, the three selected strains *P. lactis* SV9, *P. paracarnis* S45 and *P. polymyxa* SV13 have potentially different modes of actions as *P. polymyxa* SV13 inhibited Fmed growth mainly by diffusible metabolites, and *P. lactis* SV9 via the production of volatile metabolites. *P. paracarnis* S45 inhibited the growth of Fmed through both diffusible and volatile metabolites. According to the literature, when bacteria from these genera were tested against GTD-pathogens, antibiosis and induction of grapevine resistance were identified as the main mechanisms of action employed (Yang et al., 2011; Haidar et al., 2016; Li and Chen, 2019; Dutta et al., 2020; Mesguida et al., 2023). Besides, persistence and efficacy of biocontrol agents under field conditions depend on their ability to colonize plant tissues, and to resist to various biotic and abiotic stresses (Bardin et al., 2015; Mesguida et al., 2023). The presence of AMR genes has already been reported in some biocontrol agents such as *Trichoderma* spp. and *Clonostachys* spp. (Ruocco et al., 2009; Broberg et al., 2021). The detection of AMR genes in the genomes of the selected bacterial strains underscores the necessity for more extensive analyses, alongside ecotoxicological studies to evaluate the safety of these strains before proceeding with any potential registration and commercialization.

The genomic analysis of the three BCAs strains studied here, revealed that different CAZymes, mainly GT and GH are dominant. This may indicate versatile carbohydrate metabolization (Cragg et al., 2015), Additionally, the presence of genes associated with resistance to various biotic stresses and plant antimicrobial substances may enhance their ability to colonize diverse ecosystems, allowing these strains to outcompete pathogens for space and nutrients. Furthermore, these strains harbor gene clusters which encode function related to neutralizing abiotic stresses, such as temperature fluctuations and heavy metal detoxification. Their tolerance to temperature variations makes them suitable for application under field conditions, which could enhance their resilience. Additionally, their ability to detoxify heavy metals may support their use in the integrated management of GTD pathogens.

Numerous gene clusters, involved in the synthesis of biocontrol metabolites were identified in the genomes of the two *Pseudomonas* strains S45 and SV9, and are related to the biosynthesis of the arylpolyene, APE Vf. These metabolites have been previously reported as antifungal metabolites in *Pseudomonas fluorescens* (Dutta et al., 2020). Additionally, *Pseudomonas* strains S45 and SV9 encode the biosynthesis of fragin and fengycin, two metabolites known for their antifungal properties (Deleu et al., 2005; Sieber et al., 2020). The antagonistic activity of fragin is mainly due to its ability to chelate metals, potentially inhibiting various enzymes by binding to their metallic cofactors. While fengycin, a lipopeptide, inhibits cell wall biosynthesis (Deleu et al., 2005; Sieber et al., 2020). *P. lactis* SV9 encodes the biosynthesis of rhizomide, an antifungal metabolite previously reported by Lepetit et al., (2023). *P. polymyxa* SV13 encodes different antifungal metabolites including, paenithipeptin, polymyxin and fusaricidin. Among these, fusaricidin was found to be the most abundantly produced metabolite by SV13 in the presence of Fmed in our metabolomic study. It is hypothesized that the antifungal mechanisms of polymyxin and fusaricidin are related to their ability to disrupt the integrity of the cytoplasmic membrane (Li and Chen, 2019; Xue et al., 2022; Zhai et al., 2010). Additionally, fusaricidin has the capacity to inhibit pathogen spore germination and induce systemic resistance against *Fusarium* Wilt in cucumber (Li and Chen, 2019). We further identified xenocoumacin 1, in the metabolome of *P. polymyxa* SV13, a metabolite previously reported to exhibit antifungal activity against *Phytophthora* (Yang et al., 2011; Zhou et al., 2017). Bacilysin, another antifungal metabolite (Wang et al., 2018), was detected in the metabolomes of *P. paracarnis* S45 and *P. lactis* SV9. It was shown that its antifungal activity was related to the inhibition of glucosamine-6-phosphate synthase, which is an ubiquitous enzyme of primary anabolism that represent an attractive target for the development of antimicrobial compounds (Stefaniak et al., 2022). The two *Pseudomonas* strains SV9 and S45 produce N-Butyryl-L-homoserinelactone (C4-HSL), which is a quorum sensing signal molecule that is commonly used in gram-negative bacteria to coordinate the behavior of the bacterial community (Song et al., 2011; Viswanath et al., 2020), but also to significantly enhance root growth in *Arabidopsis thaliana* (Von Rad U et al., 2008).

The volatolome has also been studied in order to find potential biocontrol metabolites. *P. lactis* SV9 and *P. paracarnis* S45 exhibited high effectiveness in inhibiting Fmed growth, with inhibition rates of 96 % and 87 %, respectively. We showed that DMDS was the main metabolite produced by the two *Pseudomonas* strains S45 and SV9. Our findings demonstrate that pure DMDS effectively inhibit the growth of Fmed on its pure form. However, the inhibition observed with this metabolite alone was lower compared to the inhibition achieved in the VOCs assay with both *Pseudomonas* strains. This suggests that other metabolites, beyond DMDS, may contribute to the inhibition of Fmed. DMDS is a volatile organic compound produced by various bacterial strains, which causes strong antifungal activity against phytopathogenic fungi (Bhunia and Meshram, 2022; Elkahoui et al., 2015; Tyagi et al., 2020). According to Tyagi et al. (2020), DMDS inhibited *Sclerotinia minor* by damaging its cell membranes (Tyagi et al., 2020). On plants, Meldau et al. (2013) reported that DMDS promoted the growth of *Nicotiana attenuata* under sulfur limiting conditions (Meldau et al., 2013) suggesting its potential to stimulate the plant's growth alongside its antifungal properties.

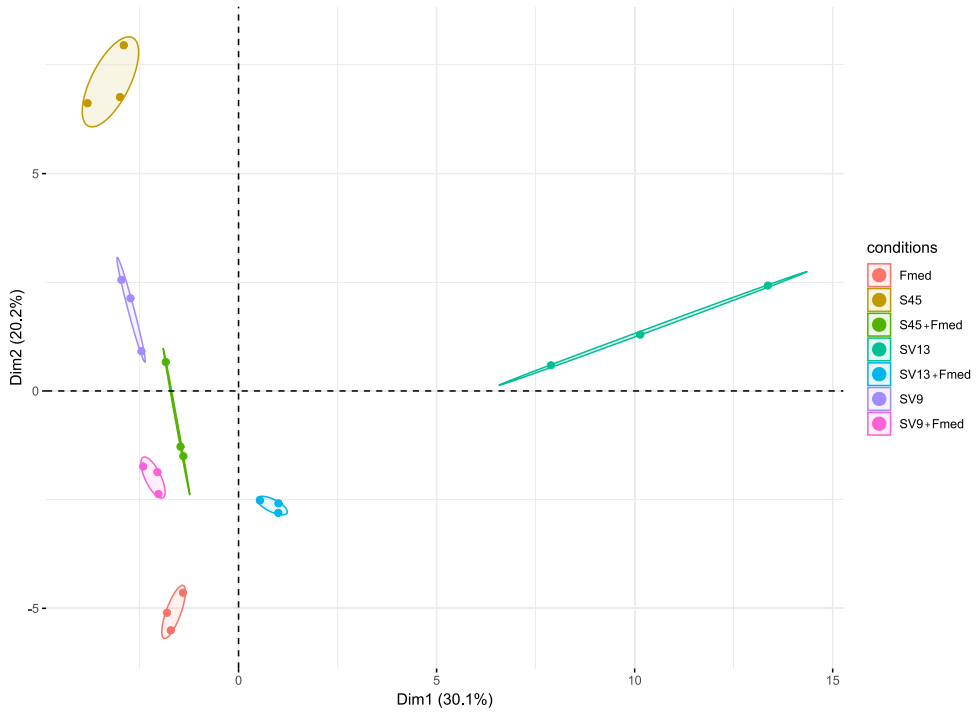

Fig. 10. Principal Coordinate Analysis (PCoA) of the volatolomic profile of *Pseudomonas lactis* SV9, *Pseudomonas paracarnis* S45 and *Paenibacillus polymyxa* SV13, when cultivated alone or with *Fomitiporia mediterranea*.

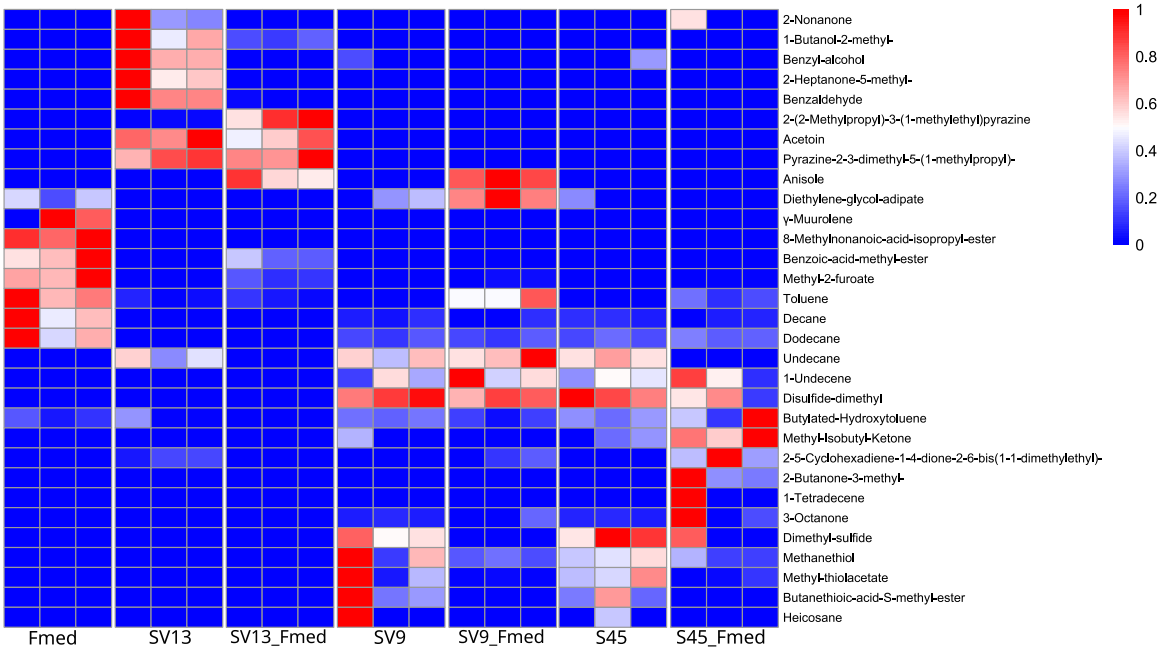

Fig. 11. Volatile organic compounds (VOCs) from *Fomitiporia mediterranea*, and the three bacterial strains *Pseudomonas lactis* SV9, *Pseudomonas paracarnis* S45 and *Paenibacillus polymyxa* SV13 when cultivated alone and with *Fomitiporia mediterranea*. Columns represent the VOCs profiles of the different microorganism for each condition. Rows represent the 31 VOCs selected (Blue, low abundance; red, high abundance).

Regarding other metabolites, both *Pseudomonas* strains S45 and SV9 produced 1-undecene in higher quantities in the presence of Fmed. Previous research showed that 1-undecene was the main metabolite produced by different *Pseudomonas* species and has a strong antifungal activity toward various fungal pathogens (Cordero et al., 2014; Hunziker et al., 2015; Tagele et al., 2019; Velivelli et al., 2015). Additionally *P. paracarnis* S45 produced 1-tetradecene in the presence of Fmed, which has been reported to have antimicrobial properties (Ajijah et al., 2023; Lammers et al., 2021). This suggests that both 1-undecene and 1-tetradecene may play roles in the inhibition of Fmed growth.

5. Conclusion

The literature is rich in issues related to the inconsistent effectiveness of biocontrol agents between *in vitro* and field conditions. Combining different mode of actions such as antibiotic production and plant defense

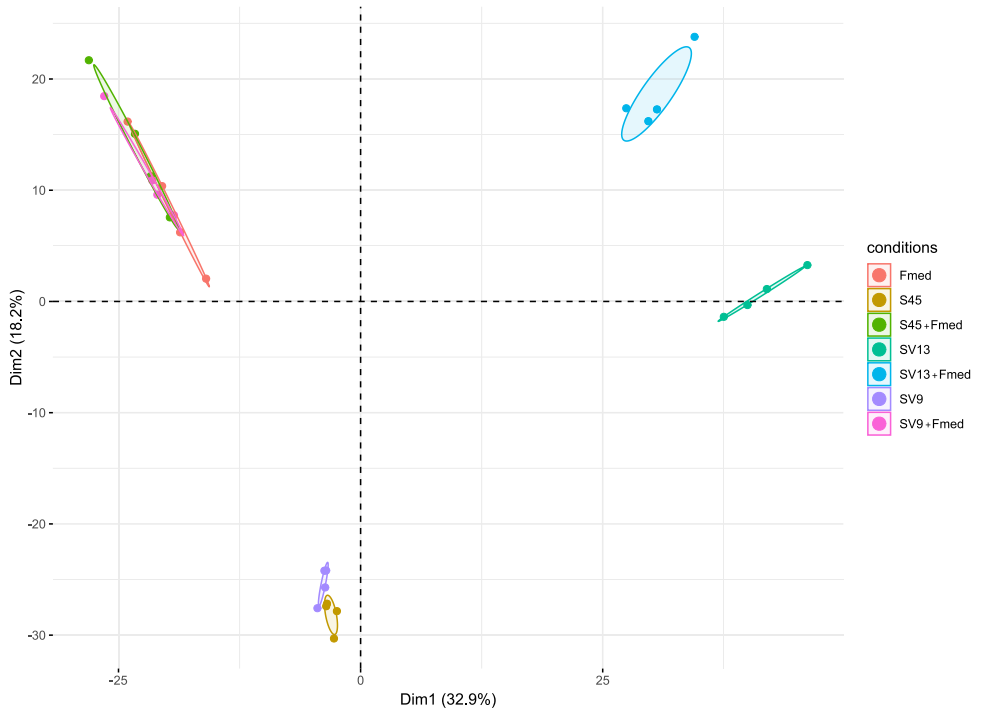

Fig. 12. Principal Coordinate Analysis (PCoA) of the metabolomic profiles of *Pseudomonas paracarnis* S45, *Pseudomonas lactis* SV9 and *Paenibacillus polymyxa* SV13, when cultivated alone or with *Fomitiporia mediterranea*.

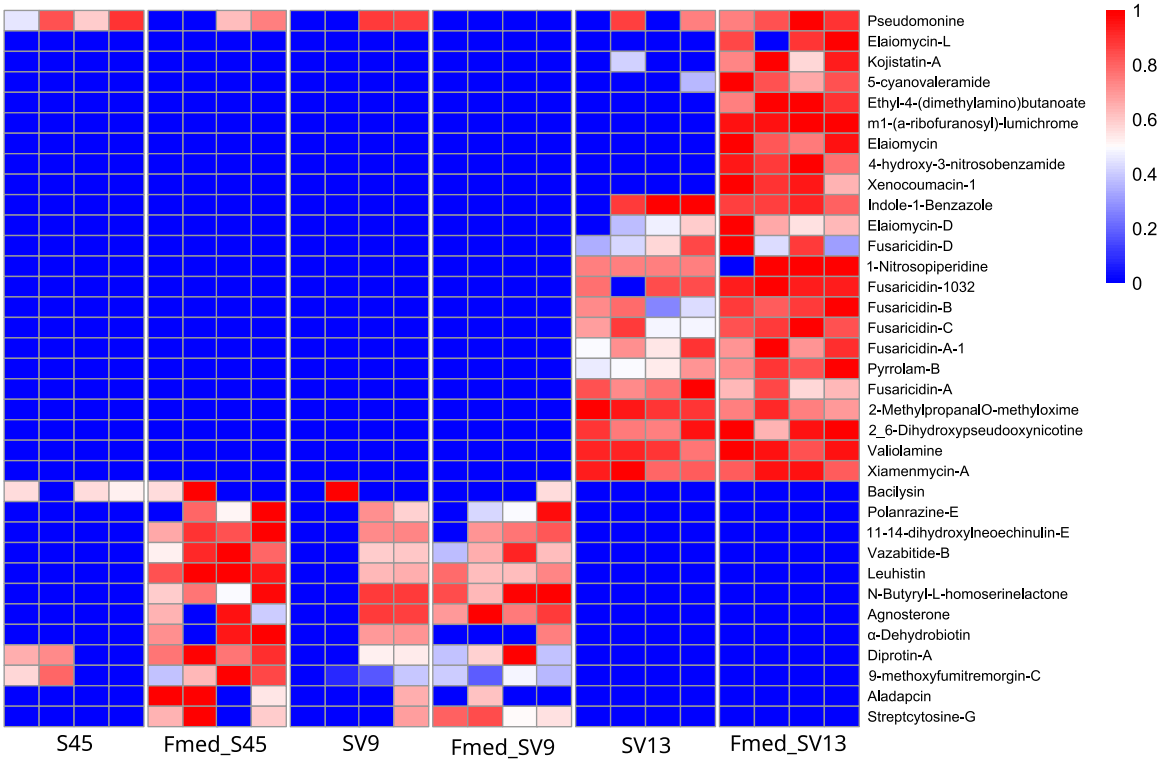

Fig. 13. Antifungal metabolites from the bacterial strains *Pseudomonas paracarnis* S45, *Pseudomonas lactis* SV9 and *Paenibacillus polymyxa* SV13 which are over expressed in the condition of the coculture of *Fomitiporia mediterranea* with the biocontrol bacteria (ratio >/= 1.2). Columns represent the profiles of the different microorganism for each condition. Rows represent the selected metabolites (Blue, low abundance; red, high abundance).

stimulation, potentially offers a more robust and durable biocontrol solution. In our study, we identified three antagonistic bacterial strains that exhibit significant inhibitory effects against *Fomitiporia mediterranea* (Fmed). Our findings highlight the diverse mechanisms employed by these biocontrol agents. The two *Pseudomonas* strains, *P. lactis* SV9 and *P. paracarnis* S45, primarily suppress Fmed growth through the production of volatile organic compounds, such as the antifungal compound dimethyl disulfide (DMDS) which is the most

abundant metabolite identified. On the other hand, *P. polymyxa* SV13 effectively inhibits Fmed by producing extracellular metabolites, including fusaricidin-type compounds known for their antifungal properties. The synergistic combination of these strains may further amplify their effectiveness as they act through different modes of actions. The metabolomic and genomic analysis enabled the identification of antifungal metabolites along with gene clusters that encode for metabolites with antifungal activities. Most of these metabolites target the cell wall e.g., polymyxin, fusaricidin, fengycin, chitinase, while others inhibit vital enzymatic activities e.g., fragin. These bacterial isolates also produce siderophores, which allow them to compete with pathogens for iron e.g., pseudomonine. All these enable direct mechanisms of action. Additionally, the three selected strains are able to act by indirect mechanisms through induction of the plant systemic resistance, nitrogen fixation and phosphorus solubilization, and the promotion of the plant growth. Whole genome analysis revealed that these strains possess genes associated with the regulation of various abiotic stresses, such as tolerance to extreme temperatures and resistance to heavy metals like copper, commonly used in agriculture. These characteristics make them strong candidates for field trials as biocontrol agents, either used alone or as part of integrated management strategies.

Funding

This work was supported by the Excellence Initiative of Université de Pau et des Pays de l'Adour–I-Site E2S UPPA [Project Biovine, seed funding], a French "Investissements d'Avenir" program and by the Industrial Chair "WinEsca" funded by the ANR (French National Research Agency, grant number ANR-22CHIN-0002-01), and the JAs Hennessy & Co and GreenCell companies. OM salary was funded by GreenCell.

Author statement

OM conceptualized, performed the experiments, analyzed the data and prepared the first version of the manuscript; SC, AW and LA conducted the acquisition and interpretation of genomic data; SG and RL designed and guided the acquisition of LC-MS/MS data; MLB and MT designed and performed SPME-GC MS experiments; AT, ADZ and JYB supervised the research and revised the manuscript; RG, PR and EA contributed to obtaining the funding for this study, they supervised the work, and contributed to the writing of the manuscript. All the authors read and approved the final version of the manuscript.

CRediT authorship contribution statement

Le Bechec Mickaël: Writing – review & editing, Software, Methodology, Conceptualization. **Godin Simon:** Writing – review & editing, Software, Methodology, Formal analysis. **Taibi Ahmed:** Resources. **Terrasse Maxence:** Software, Methodology, Formal analysis. **Rey Patrice:** Writing – review & editing, Supervision, Project administration, Investigation, Funding acquisition, Conceptualization. **Wallner Adrian:** Writing – review & editing, Software, Methodology, Formal analysis. **Attard Eléonore:** Writing – review & editing, Supervision, Project administration, Investigation, Funding acquisition, Conceptualization. **Compant Stéphane:** Writing – review & editing, Supervision, Software, Investigation, Data curation. **Lobinski Ryszard:** Writing – review & editing, Methodology, Conceptualization. **Antonielli Livio:** Writing – review & editing, Software, Methodology, Formal analysis. **Dreux-Zigha Assia:** Writing – review & editing, Supervision, Project administration, Conceptualization. **Guyoneaud Rémy:** Writing – review & editing, Supervision, Funding acquisition, Conceptualization. **Mesguida Ouiza:** Writing – original draft, Visualization, Validation, Software, Methodology, Investigation, Formal analysis, Data curation. **Berthon Jean-Yves:** Project administration, Funding acquisition.

Acknowledgements

We are grateful to Ange ANGAITS and Thierry PIGOT from, Universite de Pau et des Pays de l'Adour, CNRS, IPREM, Pau, France, for their valuable advice and support in developing our metabolomic analysis protocols. We thank Amira YACOUB, Rana HAIDAR and Fanny GUEDEA for their assistance with experimental procedures and Renaud TRAVADON for his help with LC-MS data analysis.

Appendix A. Supporting information

Supplementary data associated with this article can be found in the online version at doi:10.1016/j.micres.2025.128085.

Data Availability

Data will be made available on request.

References

Ajijah, N., Fiodor, A., Dziurzynski, M., Stasiuk, R., Pawlowska, J., Dziewit, L., Pranaw, K., 2023. Biocontrol potential of *Pseudomonas protegens* ML15 against Botrytis cinerea causing gray mold on postharvest tomato (*Solanum lycopersicum* var. cerasiforme). Front. Plant Sci. 14, 1288408. https://doi.org/10.3389/fpls.2023.1288408.

Alexander, D.B., Zuberer, D.A., 1991. Use of chrome azurol S reagents to evaluate siderophore production by rhizosphere bacteria. Biol. Fertil. Soils 12, 39–45. https://doi.org/10.1007/BF00369386.

Antonielli, L., Großkinsky, D.K., Koch, H., Trognitz, F., Sanchez Mejia, A., Nagel, M., 2024. BacFlux: a workflow for bacterial short reads assembly, QC, annotation, and more. Zenodo. https://doi.org/10.5281/zenodo.11143917.

Aziz, R.K., Bartels, D., Best, A.A., DeJongh, M., Disz, T., Edwards, R.A., Formsma, K., Gerdes, S., Glass, E.M., Kubal, M., Meyer, F., Olsen, G.J., Olson, R., Osterman, A.L., Overbeek, R.A., McNeil, L.K., Paarmann, D., Paczian, T., Parrello, B., Pusch, G.D., Reich, C., Stevens, R., Vassieva, O., Vonstein, V., Wilke, A., Zagnitko, O., 2008. The RAST server: rapid annotations using subsystems technology. BMC Genom. 9, 75. https://doi.org/10.1186/1471-2164-9-75.

Bağcı, C., Diamond, S., Megan, M., 2021. Fast and easy taxonomic and functional analysis of short and long microbiome sequences. Curr. Protoc. 1 (1), e99. https://doi.org/10.1002/cpr.99.

Bardin, M., Ajouz, S., Comby, M., Lopez-Ferber, M., Graillot, B., Siegwart, M., Nicot, P.C., 2015. Is the efficacy of biological control against plant diseases likely to be more durable than that of chemical pesticides? Front. Plant Sci. 6. https://doi.org/10.3389/fpls.2015.00566.

Bertsch, C., Ramírez-Suero, M., Magnin-Robert, M., Larignon, P., Chong, J., Abou-Mansour, E., Spagnolo, A., Clément, C., Fontaine, F., 2013. Grapevine trunk diseases: complex and still poorly understood: Grapevine trunk diseases. Plant Pathol. 62, 243–265. https://doi.org/10.1111/j.1365-3059.2012.02674.x.

Bhunia, S., Meshram, S., 2022. A review on detailed understanding and recent advances of biocontrol agent: *Pseudomonas fluorescens*. Ecol. Environ. Conserv. S185–S195. https://doi.org/10.53550/EEC.2022.v28i06s.031.

Blin, K., Shaw, S., Augustijn, H.E., Reitz, Z.L., Biermann, F., Alanjary, M., Fetter, A., Terlouw, B.R., Metcalf, W.W., Helfrich, E.J.N., van Wezel, G.P., Medema, M.H., Weber, T., 2023. antiSMASH 7.0: new and improved predictions for detection, regulation, chemical structures and visualisation. Nucleic Acids Res. 51, W46–W50. https://doi.org/10.1093/nar/gkad344.

Broberg, M., Dubey, M., Iqbal, M., Gudmundssson, M., Ihrmark, K., Schroers, H., Funck Jensen, D., Brandström Durling, M., Karlsson, M., 2021. Comparative genomics highlights the importance of drug efflux transporters during evolution of mycoparasitism in *Clonostachys* subgenus *Bionectria* (Fungi, Ascomycota, Hypocreales). Evolut. Appl. 14, 476–497. https://doi.org/10.1111/eva.13134.

Bruez, E., Vallance, J., Gerbore, J., Lecomte, P., Da Costa, J.-P., Guerin-Dubrana, L., Rey, P., 2014. Analyses of the temporal dynamics of fungal communities colonizing the healthy wood tissues of esca leaf-symptomatic and asymptomatic vines. PLoS ONE 9, e95928. https://doi.org/10.1371/journal.pone.0095928.

Bruez, E., Vallance, J., Gautier, A., Laval, V., Compant, S., Maurer, W., Sessitsch, A., Lebrun, M., Rey, P., 2020. Major changes in grapevine wood microbiota are associated with the onset of esca, a devastating trunk disease. Environ. Microbiol. 22, 5189–5206. https://doi.org/10.1111/1462-2920.15180.

Bruno, G., Ippolito, M., Bragazzi, L., Tommasi, F., 2020. Physiological response of 'Italia' grapevine to some "Esca complex"-associated fungi (preprint). Preprints. https://doi.org/10.22541/au.159545220.08380919.

Cholet, C., Bruez, É ., Lecomte, P., Barsacq, A., Martignon, T., Giudici, M., Simonit, M., Dubourdieu, D., Gény, L., 2021. Plant resilience and physiological modifications induced by curettage of Esca-diseased grapevines. OENO One 55, 153–169. https://doi.org/10.20870/oeno-one.2021.55.1.4478.

Cordero, P., Príncipe, A., Jofré, E., Mori, G., Fischer, S., 2014. Inhibition of the phytopathogenic fungus Fusarium proliferatum by volatile compounds produced by *Pseudomonas*. Arch. Microbiol. 196, 803–809. https://doi.org/10.1007/s00203-014-1019-6.

Cragg, S.M., Beckham, G.T., Bruce, N.C., Bugg, T.D., Distel, D.L., Dupree, P., Etxabe, A. G., Goodell, B.S., Jellison, J., McGeehan, J.E., McQueen-Mason, S.J., Schnorr, K., Walton, P.H., Watts, J.E., Zimmer, M., 2015. Lignocellulose degradation mechanisms across the Tree of Life. Curr. Opin. Chem. Biol. 29, 108–119. https://doi.org/10.1016/j.cbpa.2015.10.018.

Csótó, A., Nagy, A., Laurinyecz, N., Nagy, Z.A., Németh, C., Németh, E.K., Csikász-Krizsics, A., Rakonczás, N., Fontaine, F., Fekete, E., Flipphi, M., Karaffa, L., Sándor, E., 2023. Hybrid vitis cultivars with American or Asian ancestries show higher tolerance towards grapevine trunk diseases. Plants 12, 2328. https://doi.org/10.3390/plants12122328.

Del Frari, G., Cabral, A., Nascimento, T., Boavida Ferreira, R., Oliveira, H., 2019. Epicoccum layuense a potential biological control agent of esca-associated fungi in grapevine. PLoS ONE 14, e0213273. https://doi.org/10.1371/journal.pone.0213273.

Deleu, M., Paquot, M., Nylander, T., 2005. Fengycin interaction with lipid monolayers at the air–aqueous interface—implications for the effect of fengycin on biological membranes. J. Colloid Interface Sci. 283, 358–365. https://doi.org/10.1016/j.jcis.2004.09.036.

Dutta, S., Yu, S.-M., Lee, Y.H., 2020. Assessment of the contribution of antagonistic secondary metabolites to the antifungal and biocontrol activities of *Pseudomonas fluorescens* NBC275. Plant Pathol. J. 36, 491–496. https://doi.org/10.5423/PPJ.FT.08.2020.0149.

Elkahoui, S., Djébali, N., Yaich, N., Azaiez, S., Hammami, M., Essid, R., Limam, F., 2015. Antifungal activity of volatile compounds-producing *Pseudomonas* P2 strain against *Rhizoctonia solani*. World J. Microbiol. Biotechnol. 31, 175–185. https://doi.org/10.1007/s11274-014-1772-3.

European Food Safety Authority (EFSA, 2024. EFSA statement on the requirements for whole genome sequence analysis of microorganisms intentionally used in the food chain. EFS2 22. https://doi.org/10.2903/j.efsa.2024.8912.

Fischer, M., 2002. A new wood-decaying basidiomycete species associated with esca of grapevine: *Fomitiporia mediterranea* (Hymenochaetales). Mycol. Prog. 1, 315–324. https://doi.org/10.1007/s11557-006-0029-4.

Fontaine, F., Gramaje, D., Armengol, J., Smart, R., Nagy, Z.A., Borgo, M., Rego, C., Corio-Costet, M.-F., 2016. Grapevine trunk diseases. A Rev. 26.

Gastou, P., Irvine, A.D., Arcens, C., Courchinoux, E., This, P., Leeuwen, C.V., Delmas, C.E. L., 2024. large gradient of susceptibility to esca disease revealed by long-term monitoring of 46 grapevine cultivars in a common garden vineyard.

Haidar, R., Deschamps, A., Roudet, J., Calvo-Garrido, C., Bruez, E., Rey, P., Fermaud, M., 2016. Multi-organ screening of efficient bacterial control agents against two major pathogens of grapevine. Biol. Control 92, 55–65. https://doi.org/10.1016/j.biocontrol.2015.09.003.

Haidar, R., Yacoub, A., Vallance, J., Compant, S., Antonielli, L., Saad, A., Habenstein, B., Kauffmann, B., Grélard, A., Loquet, A., Attard, E., Guyoneaud, R., Rey, P., 2021. Bacteria associated with wood tissues of Esca-diseased grapevines: functional diversity and synergy with *Fomitiporia mediterranea* to degrade wood components. Environ. Microbiol., 1462-2920.15676 https://doi.org/10.1111/1462-2920.15676.

Haidar, R., Compant, S., Robert, C., Antonielli, L., Yacoub, A., Grélard, A., Loquet, A., Brader, G., Guyoneaud, R., Attard, E., Rey, P., 2024. Two *Paenibacillus* spp. strains promote grapevine wood degradation by the fungus *Fomitiporia mediterranea*: from degradation experiments to genome analyses. Sci. Rep. 14, 15779. https://doi.org/10.1038/s41598-024-66620-x.

Hervé, V., Ketter, E., Pierrat, J.-C., Gelhaye, E., Frey-Klett, P., 2016. Impact of *Phanerochaete chrysosporium* on the functional diversity of bacterial communities associated with decaying wood. PLoS ONE 11, e0147100. https://doi.org/10.1371/journal.pone.0147100.

Huerta-Cepas, J., Szklarczyk, D., Forslund, K., Cook, H., Heller, D., Walter, M.C., Rattei, T., Mende, D.R., Sunagawa, S., Kuhn, M., Jensen, L.J., von Mering, C., Bork, P., 2016. eggNOG 4.5: a hierarchical orthology framework with improved functional annotations for eukaryotic, prokaryotic and viral sequences. Nucleic Acids Res. 44, D286–D293. https://doi.org/10.1093/nar/gkv1248.

Hunziker, L., Bönisch, D., Groenhagen, U., Bailly, A., Schulz, S., Weisskopf, L., 2015. *Pseudomonas* strains naturally associated with potato plants produce volatiles with high potential for inhibition of *Phytophthora infestans*. Appl. Environ. Microbiol. 81, 821–830. https://doi.org/10.1128/AEM.02999-14.

Köhl, J., Medeiros, F.H.V., Lombaers-van Der Plas, C., Groenenboom-de Haas, L., Van Den Bosch, T., 2020. Efficacies of bacterial and fungal isolates in biocontrol of Botrytis cinerea and *Pseudomonas syringae* pv. tomato and growth promotion in tomato do not correlate. Biol. Control 150, 104375. https://doi.org/10.1016/j.biocontrol.2020.104375.

Lammers, A., Zweers, H., Sandfeld, T., Bilde, T., Garbeva, P., Schramm, A., Lalk, M., 2021. Antimicrobial compounds in the volatilome of social spider communities. Front. Microbiol. 12, 700693. https://doi.org/10.3389/fmicb.2021.700693.

Lepetit, C.A., Paquette, A.R., Brazeau-Henrie, J.T., Boddy, C.N., 2023. Total and chemoenzymatic synthesis of the lipodepsipeptide rhizomide A. Bioorg. Med. Chem. Lett. 96, 129506. https://doi.org/10.1016/j.bmcl.2023.129506.

Li, Y., Chen, S., 2019. Fusaricidin produced by *Paenibacillus polymyxa* WLY78 induces systemic resistance against fusarium wilt of cucumber. Int. J. Mol. Sci. 20, 5240. https://doi.org/10.3390/ijms20205240.

Lombard, V., Golaconda Ramulu, H., Drula, E., Coutinho, P.M., Henrissat, B., 2014. The carbohydrate-active enzymes database (CAZy) in 2013. Nucleic Acids Res. 42, D490–D495. https://doi.org/10.1093/nar/gkt1178.

Mannerucci, F., D'Ambrosio, G., Regina, N., Schiavone, D., Bruno, G.L., 2023. New potential biological limiters of the main esca-associated fungi in grapevine. Microorganisms 11, 2099. https://doi.org/10.3390/microorganisms11082099.

Martínez-Diz, M. del P., Eichmeier, A., Spetik, M., Bujanda, R., Díaz-Fernández, Á., Díaz-Losada, E., Gramaje, D., 2020. Grapevine pruning time affects natural wound colonization by wood-invading fungi. Fungal Ecol. 48, 100994. https://doi.org/10.1016/j.funeco.2020.100994.

Meldau, D.G., Meldau, S., Hoang, L.H., Underberg, S., Wunsche, H., Baldwin, I.T., 2013. Dimethyl disulfide produced by the naturally associated bacterium *Bacillus* sp. B55 Promotes *Nicotiana attenuata* growth by enhancing sulfur nutrition. Plant Cell 25, 2731–2747. https://doi.org/10.1105/tpc.113.114744.

Mesguida, O., Haidar, R., Yacoub, A., Dreux-Zigha, A., Berthon, J.-Y., Guyoneaud, R., Attard, E., Rey, P., 2023. Microbial biological control of fungi associated with grapevine trunk diseases: a review of strain diversity, modes of action, and advantages and limits of current strategies. J. Fungi 9, 638. https://doi.org/10.3390/jof9060638.

Mondello, V., Songy, A., Battiston, E., Pinto, C., Coppin, C., Trotel-Aziz, P., Clément, C., Mugnai, L., Fontaine, F., 2018b. Grapevine trunk diseases: a review of fifteen years of trials for their control with chemicals and biocontrol agents. Plant Dis. 102, 1189–1217. https://doi.org/10.1094/PDIS-08-17-1181-FE.

Mondello, V., Larignon, P., Armengol, J., Kortekamp, A., Vaczy, K., Prezman, F., Serrano, E., Rego, C., Mugnai, L., Fontaine, F., 2018a. Management of grapevine trunk diseases: knowledge transfer, current strategies and innovative strategies adopted in Europe. Phytopathol. Mediterr. 57. https://doi.org/10.14601/Phytopathol_Mediterr-23942.

Mondello, V., Spagnolo, A., Larignon, P., Clément, C., Fontaine, F., 2019. Phytoprotection potential of *Fusarium proliferatum* for control of Botryosphaeria dieback pathogens in grapevine. Phytopathol. Mediterr. 58, 295–308. https://doi.org/10.14601/Phytopathol_Mediter-10617.

Moretti, S., Pacetti, A., Pierron, R., Kassemeyer, H.-H., Fischer, M., Péros, J.-P., Perez-Gonzalez, G., Bieler, E., Schilling, M., Di Marco, S., Gelhaye, E., Mugnai, L., Bertsch, C., Farine, S., 2021. Fomitiporia mediterranea M. Fisch., the historical Esca agent: a comprehensive review on the main grapevine wood rot agent in Europe. Phytopathol. Mediterr. 60, 351–379. https://doi.org/10.36253/phyto-13021.

Murray, A.C., Woodward, S., 2007. Temporal changes in functional diversity of culturable bacteria populations in Sitka spruce stumps. For. Pathol. 37, 217–235. https://doi.org/10.1111/j.1439-0329.2007.00490.x.

Patz, S., Rauh, M., Gautam, A., Huson, D.H., 2024. mgPGPT: Metagenomic analysis of plant growth-promoting traits. https://doi.org/10.1101/2024.02.17.580828.

Ouadi, L., Bruez, E., Bastien, S., Yacoub, A., Coppin, C., Guérin-Dubrana, L., Fontaine, F., Domec, J.-C., Rey, P., 2021. Sap flow disruption in grapevine is the early signal predicting the structural, functional, and genetic responses to esca disease. Frontiers in Plant Science 12, 695846. https://doi.org/10.3389/fpls.2021.695846.

Pouzoulet, J., Pivovaroff, A.L., Santiago, L.S., Rolshausen, P.E., 2014. Can vessel dimension explain tolerance toward fungal vascular wilt diseases in woody plants? Lessons from Dutch elm disease and esca disease in grapevine. Front. Plant Sci. 5. https://doi.org/10.3389/fpls.2014.00253.

Riedle-Bauer, M., Bandion, D., Madercic, M., Gorfer, M., 2023. Activity of biocontrol agents against the grapevine pathogen *Fomitiporia mediterranea*. Phytopathol. Mediterr. 60, 213–226. https://doi.org/10.36253/phyto-14302.

Rolshausen, P.E., Greve, L.C., Labavitch, J.M., Mahoney, N.E., Molyneux, R.J., Gubler, W.D., 2008. Pathogenesis of *Eutypa lata* in grapevine: identification of virulence factors and biochemical characterization of cordon dieback. Phytopathology® 98, 222–229. https://doi.org/10.1094/PHYTO-98-2-0222.

Ruocco, M., Lanzuise, S., Vinale, F., Marra, R., Turrà, D., Woo, S.L., Lorito, M., 2009. Identification of a new biocontrol gene in *Trichoderma atroviride*: the role of an ABC transporter membrane pump in the interaction with different plant-pathogenic fungi. Mol. Plant-Microbe Interact. 22, 291–301. https://doi.org/10.1094/MPMI-22-3-0291.

Sieber, S., Daeppen, C., Jenul, C., Mannancherril, V., Eberl, L., Gademann, K., 2020. Biosynthesis and structure–activity relationship investigations of the diazeniumdiolate antifungal agent fragin. ChemBioChem 21, 1587–1592. https://doi.org/10.1002/cbic.201900755.

Song, S., Jia, Z., Xu, J., Zhang, Z., Bian, Z., 2011. N-butyryl-homoserine lactone, a bacterial quorum-sensing signaling molecule, induces intracellular calcium elevation in Arabidopsis root cells. Biochem. Biophys. Res. Commun. 414, 355–360. https://doi.org/10.1016/j.bbrc.2011.09.076.

Songy, A., Fernandez, O., Clément, C., Larignon, P., Fontaine, F., 2019. Grapevine trunk diseases under thermal and water stresses. Planta 249, 1655–1679. https://doi.org/10.1007/s00425-019-03111-8.

Stefaniak, J., Nowak, M.G., Wojciechowski, M., Milewski, S., Skwarecki, A.S., 2022. Inhibitors of glucosamine-6-phosphate synthase as potential antimicrobials or antidiabetics – synthesis and properties. J. Enzym. Inhib. Med. Chem. 37, 1928–1956. https://doi.org/10.1080/14756366.2022.2096018.

Surico, G., Mugnai, L., Marchi, G., 2006. Older and more recent observations on esca: a critical overview. Phytopathol. Mediterr. 45, 19.

Tagele, S.B., Lee, H.G., Kim, S.W., Lee, Y.S., 2019. Phenazine and 1-undecene producing *Pseudomonas chlororaphis* subsp. aurantiaca Strain KNU17Pc1 for growth promotion and disease suppression in Korean maize cultivars. J. Microbiol. Biotechnol. 29, 66–78. https://doi.org/10.4014/jmb.1808.08026.

Teather, R.M., Wood, P.J., 1982. Use of Congo red-polysaccharide interactions in enumeration and characterization of cellulolytic bacteria from the bovine rumen. Appl. Environ. Microbiol. 43 (4), 777–780.

Tyagi, S., Lee, K.-J., Shukla, P., Chae, J.-C., 2020. Dimethyl disulfide exerts antifungal activity against *Sclerotinia minor* by damaging its membrane and induces systemic resistance in host plants. Sci. Rep. 10, 6547. https://doi.org/10.1038/s41598-020-63382-0.

Ulrich, A., Klimke, G., Wirth, S., 2008. Diversity and Activity Of Cellulose-decomposing Bacteria, Isolated From A Sandy And A Loamy Soil After Long-term Manure Application. Microb. Ecol. 55, 512–522. https://doi.org/10.1007/s00248-007-9296-0.

Valtaud, C., Larignon, P., Roblin, G., Fleurat-Lessard, P., 2009. Developmental and ultrastructural features of *Phaeomoniella chlamydospora* and *Phaeoacremonium aleophilum* in relation to xylem degradation in esca disease of the grapevine. J. Plant Pathol. 91, 37–51.

Velivelli, S.L.S., Kromann, P., Lojan, P., Rojas, M., Franco, J., Suarez, J.P., Prestwich, B. D., 2015. Identification of mVOCs from andean rhizobacteria and field evaluation of bacterial and mycorrhizal inoculants on growth of potato in its center of origin. Microb. Ecol. 69, 652–667. https://doi.org/10.1007/s00248-014-0514-2.

Viswanath, G., Sekar, J., Ramalingam, P.V., 2020. Detection of diverse N-acyl homoserine lactone signalling molecules among bacteria associated with rice rhizosphere. Curr. Microbiol. 77, 3480–3491. https://doi.org/10.1007/s00284-020-02183-0.

von Rad, U., Klein, I., Dobrev, P.I., et al., 2008. Response of *Arabidopsis thaliana* to *N*-hexanoyl-dl-homoserine-lactone, a bacterial quorum sensing molecule produced in the rhizosphere. Planta 229, 73–85. https://doi.org/10.1007/s00425-008-0811-4.

Wang, T., Liu, X., Wu, M.-B., Ge, S., 2018. Molecular insights into the antifungal mechanism of bacilysin. J. Mol. Model. 24, 118. https://doi.org/10.1007/s00894-018-3645-4.

Xue, D., Older, E.A., Zhong, Z., Shang, Z., Chen, N., Dittenhauser, N., Hou, L., Cai, P., Walla, M.D., Dong, S.-H., Tang, X., Chen, H., Nagarkatti, P., Nagarkatti, M., Li, Y.-X., Li, J., 2022. Correlational networking guides the discovery of unclustered lanthipeptide protease-encoding genes. Nat. Commun. 13, 1647. https://doi.org/10.1038/s41467-022-29325-1.

Yang, X., Qiu, D., Yang, H., Liu, Z., Zeng, H., Yuan, J., 2011. Antifungal activity of xenocoumacin 1 from *Xenorhabdus nematophilus* var. pekingensis against *Phytophthora infestans*. World J. Microbiol. Biotechnol. 27, 523–528. https://doi.org/10.1007/s11274-010-0485-5.

Zhai, B., Zhou, H., Yang, L., Zhang, J., Jung, K., Giam, C.Z., Xiang, X., Lin, X., 2010. Polymyxin B, in combination with fluconazole, exerts a potent fungicidal effect. J. Antimicrob. Chemother. 65, 931–938. https://doi.org/10.1093/jac/dkq046.

Zhou, T., Yang, X., Qiu, D., Zeng, H., 2017. Inhibitory effects of xenocoumacin 1 on the different stages of *Phytophthora capsici* and its control effect on Phytophthora blight of pepper. BioControl 62, 151–160. https://doi.org/10.1007/s10526-016-9779-3.